

# Lawrence Berkeley National Laboratory

## Recent Work

**Title**

THE TEMPERATURE OF THIN FOILS IN ION BEAMS

**Permalink**

<https://escholarship.org/uc/item/1bc8m41v>

**Author**

Liljenzin, J.O.

**Publication Date**

1973-06-01

THE TEMPERATURE OF THIN FOILS IN ION BEAMS

J. O. Liljenzin

June 1973

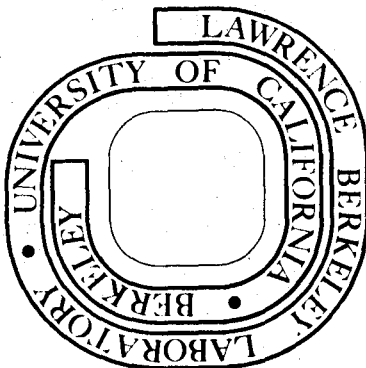
RECEIVED  
RADIATION LABORATORY

LIBRARY AND  
DOCUMENTS SECTION

Prepared for the U. S. Atomic Energy Commission  
under Contract W-7405-ENG-48

TWO-WEEK LOAN COPY

*This is a Library Circulating Copy  
which may be borrowed for two weeks.  
For a personal retention copy, call  
Tech. Info. Division, Ext. 5545*



26

## **DISCLAIMER**

This document was prepared as an account of work sponsored by the United States Government. While this document is believed to contain correct information, neither the United States Government nor any agency thereof, nor the Regents of the University of California, nor any of their employees, makes any warranty, express or implied, or assumes any legal responsibility for the accuracy, completeness, or usefulness of any information, apparatus, product, or process disclosed, or represents that its use would not infringe privately owned rights. Reference herein to any specific commercial product, process, or service by its trade name, trademark, manufacturer, or otherwise, does not necessarily constitute or imply its endorsement, recommendation, or favoring by the United States Government or any agency thereof, or the Regents of the University of California. The views and opinions of authors expressed herein do not necessarily state or reflect those of the United States Government or any agency thereof or the Regents of the University of California.

## CONTENTS

Abstract . . . . .	v
1. Calculation of the Total Amount of Beam Energy Lost in a Foil. . . . .	1
2. Cooling Methods . . . . .	2
2.1. Radiation Cooling. . . . .	2
2.2. Conduction Cooling . . . . .	2
2.3. Convection Cooling . . . . .	3
2.4. Combined Cooling. . . . .	5
3. Beam Shape and Time Function . . . . .	5
3.1. Uniform Beam Shape. . . . .	5
3.2. Gaussian Beam Shape . . . . .	6
3.3. Double-Gaussian Beam Shape. . . . .	8
4. The Foil Temperature . . . . .	9
4.1. Radiation Cooling Dominates . . . . .	9
4.1.1. Uniform beam shape. . . . .	10
4.1.2. Gaussian beam shape . . . . .	11
4.1.3. Double-Gaussian beam shape. . . . .	12
4.1.4. Calculation of the maximum temperature. . . . .	13
4.2. Conduction Cooling Dominates . . . . .	13
4.2.1. Uniform beam shape. . . . .	14
4.2.2. Gaussian beam shape . . . . .	17
4.2.3. Favorable beam shapes. . . . .	18
4.3. Convection-Cooling Dominates . . . . .	19
4.3.1. Water cooling . . . . .	19
4.3.2. Gas cooling . . . . .	20
5. Numerical Solution of the General Case . . . . .	21
5.1. Combined Radiation and Conduction Cooling . . . . .	22
Acknowledgment . . . . .	23
References . . . . .	24
Appendices	
1. Input Data for HEAT v4m1 . . . . .	25
2. Program HEAT v4m1 . . . . .	31
3. Example of the Printout from Program HEAT v4m1 . . . . .	40
Tables. . . . .	44
Figures . . . . .	47

## THE TEMPERATURE OF THIN FOILS IN ION BEAMS

J. O. Liljenzin

Lawrence Berkeley Laboratory  
University of California  
Berkeley, California 94720

June 1973

### ABSTRACT

The effect of beam-shape, pulsed operation and ion type on the temperature of thin foils in ion beams is discussed for cases where the cooling is by heat radiation, heat conduction, or convection in an external medium. Analytic solutions are given for various combinations of beam shape and cooling conditions. Nomographs are given for the estimation of the maximum temperature of thin circular foils when the cooling is either by radiation to the surroundings or by conduction to the edge of the foil. A program is described which can be used to calculate the temperature distribution at equilibrium conditions or as a function of time for arbitrarily shaped non-isotropic and non-homogeneous bodies heated internally and cooled by any combination of radiation, conduction, or convection of heat in an external gaseous medium. The heat conductivity, heat capacity, heat generation, and grayness can vary within the body; the heat conductivity and heat capacity can vary with temperature; and the heat-generation can be pulsed. Cooling by a liquid streaming on the backside of the foil is generally most effective. Radiative cooling is also dominant for very thin foils, and conduction cooling is dominant for thick foils. At a given diameter, this leads to a maximum temperature for foils with a thickness a little below the range of the ions.

## THE TEMPERATURE OF THIN FOILS IN ION BEAMS

J. O. Liljenzin

Lawrence Berkeley Laboratory  
University of California  
Berkeley, California 94720

June 1973

Thin foils are used in ion beams for stripping of the ions, degradation of beam energy, as vacuum seals, and as beam-transparent targets. Homogenous foils, made from a single substance, are used for all of the mentioned purposes. Targets are, however, often made in two layers, a backing which gives mechanical strength and impermeability for gases and a layer of the target substance which can be much thinner than the backing and lack mechanical strength.

When the beam passes through the foil it loses part of its energy by interaction with the atoms in the foil. The major part of the energy transferred from the beam to the foil occurs as heat, which must be removed to prevent the target from melting or evaporating (see Fig. 12).

### 1. CALCULATION OF THE TOTAL AMOUNT OF BEAM ENERGY LOST IN A FOIL

For sufficiently thin foils the electronic stopping power,<sup>1</sup>  $-dE/dl$ , can be assumed constant. The energy transferred to the foil per unit time,  $P_{tot}$ , can then be calculated from the relation,

$$P_{tot} \approx l \left( -\frac{dE}{dl} \right) I / Z_{eff}, \quad (1)$$

where  $l$  is the foil thickness,  $I$  the electric beam current and  $Z_{eff}$  the mean electric charge of the ions.

The electronic stopping power is no longer constant for thicker foils. The energy transferred to the foil must then be calculated from the range variation with energy.<sup>1</sup> Let  $E_0$  and  $R(E_0)$  be the energy and range in the foil material of the incident ions,  $E_l$  and  $R(E_l)$  the energy and range of the

ions after passing a layer of foil material of thickness  $l$ . The residual range,  $R(E_l)$  is computed from

$$R(E_l) = R(E_0) - l, \quad (2)$$

which gives  $E_l$ , and then  $P_{\text{tot}}$  can be calculated from

$$P_{\text{tot}} = (E_0 - E_l) \cdot I / Z_{\text{eff}}, \quad (3)$$

where  $I/Z_{\text{eff}}$  is the "particle current."

Equation (2) is most conveniently solved in a graph of  $R$  vs  $E$ , where  $E_l$  then can be read off on the energy scale.

## 2. COOLING METHODS

The heat evolved in the target can be removed by many different mechanisms, some of which are probably without interest in practical applications, i. e., removal by vaporization of the foil material, or by melting of the foil. The most useful cooling methods are cooling by heat radiation, cooling by heat conduction, and cooling by convection in an external fluid medium.

### 2.1. Radiation Cooling

When the foil surface is at a temperature,  $T_{\text{surf}}$ , which is higher than the surroundings (which are at a temperature  $T_{\text{sur}}$ ), the foil will radiate away heat with a rate per unit surface area,  $P_{\text{rad}}$ , given by Stefan's law.

$$P_{\text{rad}} = g \delta (T_{\text{surf}}^4 - T_{\text{sur}}^4), \quad (4)$$

where  $T_{\text{surf}}$  and  $T_{\text{sur}}$  are in degrees K,  $\delta$  has the value  $5.70 \times 10^{-12}$  ( $\text{W cm}^{-2}$  degree<sup>-4</sup>) and  $g$  is the grayness factor as compared to a black body ( $0 < g \leq 1$ ). The grayness factors for some common materials are listed in Table I.

### 2.2. Conduction Cooling

When an internal volume element of the foil is at a different temperature than its surroundings, heat will flow in a direction as to eliminate the temperature differences.

$$P_{\text{cond}} = \left\{ \frac{d(\lambda_x \frac{dT}{dx})}{dx} + \frac{d(\lambda_y \frac{dT}{dy})}{dy} + \frac{d(\lambda_l \frac{dT}{dl})}{dl} \right\} dV, \quad (5)$$

where  $P_{\text{cond}}$  is the heat conduction rate;  $\lambda_x$ ,  $\lambda_y$  and  $\lambda_l$  are the heat conductivities in the x, y, and l direction respectively;  $dV$  is the volume element  $dx dy dl$ . Constant values for the heat conductivities ( $\lambda$ ) can only be used in a small temperature range. For larger temperature ranges an approximation with the following equation can be used:

$$\lambda_i = a_i - b_i \cdot T + c_i \cdot T^{-2}. \quad (6)$$

Fortunately most materials are isotropic, i. e.,  $\lambda_x = \lambda_y = \lambda_l$ . Values of a, b, and c in Eq. 6 are given in Table II for some common materials.

### 2.3. Convection Cooling

The effect of convection cooling is highly dependent on the heat transfer between the foil and the cooling medium. This is usually expressed as a film-transfer coefficient  $h$  defined by

$$p_{\text{conv}} = h (T_{\text{surf}} - T_{\text{fluid}}), \quad (7)$$

where  $p_{\text{conv}}$  is the heat transfer rate per unit surface (wall area),  $h$  is the film transfer coefficient,  $T_{\text{surf}}$  is the foil surface temperature, and  $T_{\text{fluid}}$  is the fluid phase (gas or liquid) bulk temperature.

The calculation of the heat removed by convection cooling is now transformed to a problem to calculate the film-transfer coefficient ( $h$ ). This is usually solved by the application of dimensional theory to relate the actual problem to another well-investigated case for which an empirical equation is available.

The dimensionless numbers of interest when scaling and comparing film-transfer coefficients are: Reynolds number (Re), Nusselts number (Nu), and Grashofs number (Gr).<sup>2</sup> For large streaming velocities ( $Re \geq 2100$ ) with turbulent flow the value of Gr is no longer important for calculating the film-transfer coefficient.

The main problem is to find the comparable case. As a rough approximation, the foil can be thought of as a part of the wall in a circular tube. Then the following equation can be used<sup>2</sup> at low velocities and laminar flow



(Re < 2100):

$$Nu = 1.62 \sqrt[3]{\mu/\mu_f} (1 + 0.015 \sqrt[3]{Gr}) \sqrt[3]{\frac{4 w C_p}{\pi \lambda_{\text{fluid}} D}}, \quad (8)$$

where Nu and Gr are

$$Nu = h \cdot D / \lambda_{\text{fluid}}, \quad (8a)$$

$$Gr = D^3 \rho^2 \beta g (T_{\text{surf}} - T_{\text{fluid}}), \quad (8b)$$

where  $\mu$  is the viscosity of fluid at the bulk temperature,  $\mu_f$  is the viscosity of the fluid at the film mean temperature, and  $w$  is the flow rate (mass per time).  $D$  is a characteristic length (the diameter),  $\lambda_{\text{fluid}}$  is the heat conductivity of the fluid,  $\rho$  is the density of the fluid,  $\beta$  is the volume expansion coefficient,  $g$  the gravity constant, and  $C_p$  is the heat capacity of the fluid. The Grashof number reflects the increased flow due to the heating of the fluid at the surface.

For water streaming upwards, the simpler equation

$$h = (2.685 T_{\text{water}} + 51.62) \sqrt[3]{T_{\text{surf}} - T_{\text{water}}} \cdot 10^{-4} \quad (9)$$

can be used instead of (8).<sup>2</sup> Here  $T$  is in degrees centigrade and  $h$  is in  $W/cm^2 \cdot ^\circ C$ .

When the streaming velocity of the fluid is so high that turbulent flow occurs,  $Re > 10\,000$ , the following equation is valid for all fluids streaming upwards in a pipe:<sup>2</sup>

$$Nu = 0.023 (Re)^{0.8} \cdot (Pr)^{0.4}. \quad (10)$$

For liquids with  $\mu \lesssim 2$  cP and for gases with  $w \gtrsim 600 p^{2/3}$  (where  $p$  is in atm), Eq. (10) can be used almost down to  $Re = 2100$ ;  $w$  should be calculated as kg/hour. In case of a downward flow, the corresponding empirical equation is<sup>2</sup>

$$Nu = 0.023 (Re)^{0.8} \cdot (Pr)^{0.3}, \quad (11)$$

where  $Pr = C_p \mu / \lambda$ .

#### 2.4. Combined Cooling

In practice, the cooling method used is some combination of radiation cooling, conduction cooling, and convection cooling. Sometimes, depending on geometry, surface area, gas pressure, and foil temperature, one of these processes may dominate over the others. To be able to treat realistic cases, all the mentioned cooling processes must be included in the final differential equation. Assuming that heat radiation is only lost in the  $l$  direction and that the eventual surrounding fluid passes by the foil in an  $x$ - $y$  plane, the rate of heat loss by cooling,  $p_{cool}$ , can be written

$$P_{cool} = dV \left[ \frac{ng\delta}{dl} (T^4 - T_{sur}^4) + \frac{d(\lambda \frac{dT}{dx})}{dx} + \frac{d(\lambda \frac{dT}{dy})}{dy} + \frac{d(\lambda \frac{dT}{dl})}{dl} + \frac{nh}{dl} (T - T_{fluid}) \right]. \quad (12)$$

Some of the "constants" (i. e.,  $\lambda$ 's and  $h$ ) are in turn functions of  $T$  and some ( $n$  and  $g$ ) may be functions of  $x$ ,  $y$ , and  $l$ .

### 3. BEAM SHAPE AND TIME FUNCTION

The shape of the beam, i.e., the variation in beam intensity with  $x$  and  $y$  on the foil, is of great importance for the temperature distribution over the foil and thus for the maximum temperature that will occur at a given total beam current. The variation of beam current with time is also important when the cooling time-constant is less than or comparable to the frequency of the beam-current variations. Of the many possible variations of beam current with time, only two will be discussed: continuous beam and pulsed beam with fixed frequency. All beams will be assumed to be circular symmetric.

#### 3.1. Uniform Beam Shape

The beam is hitting the foil with the same intensity at all points of the surface. The power released on an area  $dA$  ( $= dx dy$ ) is then

$$P_{beam} = P_{tot} dA/A, \quad (13)$$

where  $A$  is the total exposed area of the foil.

When the beam is pulsed with a frequency  $f$  and a duty cycle of  $C$  percent,

$$t_{\text{on}} = 0.01 C/f, \quad (14)$$

$$t_{\text{off}} = (1-0.01C)/f, \quad (15)$$

where  $t_{\text{on}}$  is the on time and  $t_{\text{off}}$  is the off time of each cycle.

The current during  $t_{\text{on}}$  must now be larger than in the stationary case to give the same mean current, I:

$$I_{\text{on}} = 100 I/C, \quad (16a)$$

$$I_{\text{off}} = 0.0. \quad (16b)$$

Thus in a pulsed beam,

$$P_{\text{beam, on}} = 100 P_{\text{tot}} dA/(AC), \quad (17a)$$

$$P_{\text{beam, off}} = 0.0. \quad (17a)$$

Tilting the foil against the beam will increase the total area A with a factor  $1/\sin(\phi)$ , where  $\phi$  is the angle between the foil and the beam, and thus decrease  $P_{\text{beam}}$ .

### 3.2. Gaussian Beam Shape

The beam is hitting the foil with an intensity distribution (current distribution)

$$p(r) = k \cdot e^{-(r/s)^2}, \quad (18)$$

where  $r$  is the distance from the center of the beam,  $k$  is a proportionality constant and  $s$  is a shape factor: larger  $s$ , more diffuse beam; smaller  $s$ , more focused beam.

The total power dissipated within a radius  $R$  is  $P(R)$

$$P(R) = 2\pi k \int_{r=0}^R r e^{-(r/s)^2} dr = \pi k s^2 [1 - e^{-(R/s)^2}], \quad (19)$$

where  $k$  is a proportionality constant between surface and power. The total power of the beam must be dissipated for  $R = \infty$ , thus

$$P(\infty) = P_{\text{tot}} = \pi k s^2 \quad (20)$$

and hence

$$P(R) = P_{\text{tot}} [1 - e^{-(R/s)^2}]. \quad (21)$$

When a fraction,  $\alpha$ , of the total beam is known to hit the foil within a certain radius,  $R_\alpha$ ,  $s^2$  can be obtained from the equation

$$s^2 = - \frac{R_\alpha^2}{\ln(1-\alpha)}. \quad (22)$$

Thus the Gaussian beam is defined by its total energy,  $P_{\text{tot}}$ , and a fraction,  $\alpha$ , of  $P_{\text{tot}}$  hitting within a radius  $R_\alpha$ .

The proportionality constant  $k$  is then

$$k = - \frac{P_{\text{tot}} \ln(1-\alpha)}{\pi R_\alpha^2}. \quad (23)$$

The beam hitting a unit surface area is now

$$p_{\text{beam}}(r) = - \frac{P_{\text{tot}} \ln(1-\alpha)}{\pi R_\alpha^2} e^{-r^2 \sqrt{-\ln(1-\alpha)}/R_\alpha^2}. \quad (24)$$

In the case of a pulsed beam defined by Eqs. (16a) and (16b) we obtain

$$p(r)_{\text{beam, on}} = - \frac{100 P_{\text{tot}} \ln(1-\alpha)}{\pi C R_\alpha^2} e^{-r^2 \sqrt{-\ln(1-\alpha)}/R_\alpha^2}, \quad (25a)$$

$$p(r)_{\text{beam, off}} = 0.0. \quad (25b)$$

When the beam passing through the foil,  $P_{\text{tr}}$ , is used instead of  $P_{\text{tot}}$ , the term  $-P_{\text{tot}} \ln(1-\alpha)$  should be replaced by  $-P_{\text{tr}} \ln(1-\alpha)/\alpha$  in all equations where it occurs.

### 3.3. Double-Gaussian Beam Shape

The beam is hitting the foil with an intensity distribution (current distribution)

$$p(r) = k \cdot e^{-\left(\frac{r-\bar{R}}{s}\right)^2} \quad (26)$$

where  $k$  is a proportionality constant as before and  $\bar{R}$  is the radius at which the beam intensity is highest.

The total power dissipated within a radius  $R$  is  $P(R)$ :

$$P(R) = 2\pi k \int_0^R r e^{-\left(\frac{r-\bar{R}}{s}\right)^2} = \pi k s^2 \left[ e^{-\left(\frac{R}{s}\right)^2} - e^{-\left(\frac{R-\bar{R}}{s}\right)^2} \right] + \pi^{3/2} k s \bar{R} \left[ \operatorname{erf}\left(\frac{R}{s}\right) + \operatorname{erf}\left(\frac{R-\bar{R}}{s}\right) \right], \quad (27)$$

where  $\operatorname{erf}$  is the error function. As before, the total power of the beam must be dissipated for  $R = \infty$ , thus

$$P(\infty) = P_{\text{tot}} = \pi k s^2 e^{-\left(\frac{R}{s}\right)^2} + \pi^{3/2} k s \bar{R} \left[ \operatorname{erf}\left(\frac{R}{s}\right) + 1 \right] \quad (28)$$

and thus

$$P(R) = \frac{P_{\text{tot}}}{s \cdot e^{-\left(\frac{\bar{R}}{s}\right)^2} + \sqrt{\pi} \left[ \operatorname{erf}\left(\frac{\bar{R}}{s}\right) + 1 \right]} \left\{ s \left[ e^{-\left(\frac{R}{s}\right)^2} - e^{-\left(\frac{R-\bar{R}}{s}\right)^2} \right] + \sqrt{\pi} \bar{R} \left[ \operatorname{erf}\left(\frac{R}{s}\right) - \operatorname{erf}\left(\frac{R-\bar{R}}{s}\right) \right] \right\} \quad (29)$$

is obtained with

$$k = \frac{P_{\text{tot}}}{\pi s^2 e^{-\left(\frac{\bar{R}}{s}\right)^2} + \pi^{3/2} s \bar{R} \left[ \operatorname{erf}\left(\frac{\bar{R}}{s}\right) + 1 \right]} \quad (30)$$

With this value for  $k$  the beam shape is

$$p(r)_{\text{beam}} = \frac{P_{\text{tot}}}{\pi s^2 e^{-\left(\frac{\bar{R}}{s}\right)^2} + \pi^{3/2} s \bar{R} [\text{erf}\left(\frac{\bar{R}}{s}\right) + 1]} e^{-\left(\frac{r-\bar{R}}{s}\right)^2}. \quad (31)$$

To determine  $s$  and  $\bar{R}$ , two further values of  $P(R)$  must be given, but  $\bar{R}$  will probably be defined by other conditions and hence already be known. The spread  $s$  can then be obtained from any other known condition, e.g.,  $P(0)$  known or  $P(\bar{R})$  known. Transcendental equations are generally obtained of such a form that they must be solved by numerical methods.

As before, the beam at pulsed operation is given by the two states:

$$p(r)_{\text{beam, on}} = \frac{100 P_{\text{tot}}}{C \pi s (s e^{-\left(\frac{\bar{R}}{s}\right)^2} + \sqrt{\pi} \bar{R} [\text{erf}\left(\frac{\bar{R}}{s}\right) + 1])} e^{-\left(\frac{r-\bar{R}}{s}\right)^2}, \quad (32a)$$

$$p(r)_{\text{beam, off}} = 0.0. \quad (32b)$$

#### 4. THE FOIL TEMPERATURE

The foil temperature is given by the differential equation

$$p_{\text{beam}} - p_{\text{cool}} = \rho \cdot dV \cdot C_p \frac{dT}{dt}, \quad (33)$$

where  $p_{\text{beam}}$  is given by any suitable beam shape and time function, and  $p_{\text{cool}}$  is given by Eq. (12).

No general solution to Eq. (33) is known, but for some combination of beam shape and cooling type special solutions can be obtained.

##### 4.1. Radiation Cooling Dominates

Introducing polar coordinates, we obtain the equation

$$p_{\text{beam}} = n \delta g [T_{(r,t)}^4 - T_{\text{sur}}^4] = dl \rho C_p \frac{dT_{(r,t)}}{dt}. \quad (34)$$

4.1.1. Uniform beam shape

In this case Eqs. (34) and (13) give

$$\frac{P_{tot}}{\pi R^2} - n\delta g T(r, t)^4 + n\delta g T_{sur}^4 = dl \rho C_p \frac{dT(r, t)}{dt} \quad (35)$$

The steady-state solution is obtained when  $dT(r, t)/dt = 0$ ,

$$T(r, \infty) = \sqrt[4]{T_{sur}^4 + \frac{P_{tot}}{n\delta g \pi R^2}} \quad (36)$$

where  $n$  is the number of radiating surfaces. As can be seen,  $T(r, \infty)$  in Eq. (36) is independent of  $r$ , so the surface will have the same temperature all over.<sup>3</sup>

When the beam is pulsed, however, the heat capacity of the foil will decrease the maximum temperature and increase the minimum temperature. The two differential equations valid during heating ( $t_{on}$ ) and cooling ( $t_{off}$ ) are

$$\frac{100 P_{tot}}{C \pi R^2} + n\delta g T_{sur}^4 - n\delta g T(r, t)^4 = dl \rho C_p \frac{dT(r, t)}{dt} \quad (37a)$$

for  $\frac{m}{f} \leq t \leq \frac{m}{f} + t_{on}$  where  $m = 0, 1, 2, 3, \text{ etc.}$

and

$$n\delta g T_{sur}^4 - n\delta g T(r, t)^4 = dl \rho C_p \frac{dT(r, t)}{dt} \quad (37b)$$

for  $\frac{m}{f} + t_{on} \leq t \leq \frac{m+1}{f}$ .

As  $C_p$  is a function of  $T$  very similar to Eq. (6),

$$C_p \approx a + bT + cT^{-2} \quad (38)$$

The exact solutions of Eqs. (37a) and (37b) are quite complicated functions of  $T$ . However, the third term in Eq. (38) is only important at very low temperatures where the radiation cooling is negligible in comparison with conduction and convection. Thus a linear dependence of  $C_p$  on  $T$  is sufficient. The solution is independent of  $r$  and can be written as follows:

$$t - t_0 = \frac{1}{4B^3} \left\{ A \ln \frac{[B+T(t)][B-T(t_0)]}{[B-T(t)][B+T(t_0)]} + 2A \arctan \frac{B[T(t) - T(t_0)]}{B^2 + T(t)T(t_0)} + D \ln \frac{[B^2 + T(t)^2][B^2 - T(t_0)^2]}{[B^2 - T(t)^2][B^2 + T(t_0)^2]} \right\}, \quad (39)$$

where  $B = \sqrt[4]{\frac{100 P_{\text{tot}}}{C_p R^2 n \delta g} + T_{\text{sur}}^4}$  with  $P_{\text{tot}} = 0$  for  $\frac{m}{f} + t_{\text{on}} \leq t \leq \frac{m+1}{f}$ ,  $A = d \ell \rho a / (n \delta g)$ , and

$D = d \ell \rho b / (n \delta g)$ . Figure 1 shows the temperature calculated for a frequency of 40 Hz and a typical foil. Similar results are given in Refs. 3 and 4, which however, consider  $C_p$  as a constant independent of  $T$ .

#### 4.1.2. Gaussian beam shape

Equations (34) and (24) give

$$-\frac{P_{\text{tot}} \ln(1-\alpha)}{\pi R_a^2} e^{-\frac{r^2 \sqrt{-\ln(1-\alpha)}}{R_a^2}} - n \delta g T(r, t)^4 + n \delta g T_{\text{sur}}^4 = d \ell \rho C_p \frac{dT(r, t)}{dt}. \quad (40)$$

Obviously the temperature in the center of the beam will determine the behavior of the foil. A specialization of Eq. (40) to the hottest spot on the target gives for a continuous beam

$$-\frac{P_{\text{tot}} \ln(1-\alpha)}{\pi R_a^2} - n \delta g T_{\text{max}}^4 + n \delta g T_{\text{sur}}^4 = 0. \quad (41)$$

The solution of Eq. (41) can be written as follows:

$$T_{\text{max}} = \sqrt[4]{-\frac{P_{\text{tot}} \ln(1-\alpha)}{\pi R_a^2 n \delta g} + T_{\text{sur}}^4}. \quad (42)$$



A comparison with Eq. (36), valid for uniform beam shape, shows that  $T_{\max}$  for the Gaussian beam shape is higher. When  $T_{\text{sur}}^4$  is negligible,  $T_{\max}/T(r, \infty) \approx \sqrt[4]{-\ln(1-a)}$  is obtained. So, the smaller the utilized part of the Gaussian beam is, the cooler is the foil, approaching  $T(r, \infty)$  as  $a$  goes to zero. Figure 2 shows the variation of  $T_{\max}/T(r, \infty)$  with  $a$  at equal transmitted beam intensities.

When a pulsed beam is used, the equation for the highest temperature  $T(0, t)$  is

$$-\frac{100 P_{\text{tot}} \ln(1-a)}{C \pi R_a^2} - n \delta g T(0, t)^4 + n \delta g T_{\text{sur}}^4 = d l \rho C_p \frac{dT(0, t)}{dt} \quad (43)$$

Equation (39) is a solution to Eq. 43 with

$$B = \sqrt[4]{-\frac{100 P_{\text{tot}} \ln(1-a)}{C \pi R_a^2 n \delta g} + T_{\text{sur}}^4} \quad \text{for} \quad \frac{m}{f} \leq t \leq \frac{m}{f} + t_{\text{on}},$$

$$B = 0 \quad \text{for} \quad \frac{m}{f} + t_{\text{on}} \leq t \leq \frac{m+1}{f}, \quad A = d l \rho a / (n \delta g) \quad \text{and}$$

$D = d l \rho b / n \delta g$ . About the same shapes as shown in Fig. 1 are thus obtained. Some deviation occur at beam intensities where  $T_{\text{sur}}^4$  is important in the calculation of  $B$ .

#### 4.1.3. Double-Gaussian beam shape

The differential equation for radiation cooling at a double-Gaussian beam shape is obtained from Eqs. (34) and (31).

$$\frac{P_{\text{tot}} e^{-\left(\frac{r-\bar{R}}{s}\right)^2}}{\pi s^2 e^{-\left(\frac{\bar{R}}{s}\right)^2} + \pi^{3/2} s \bar{R} [\text{erf}\left(\frac{\bar{R}}{s}\right) + 1]} - n \delta g [T(r, t)^4 - T_{\text{sur}}^4] = d l \rho C_p \frac{dT(r, t)}{dt} \quad (44)$$

The steady-state solution to Eq. (44) is

$$T(r, \infty) = \sqrt[4]{T_{\text{sur}}^4 + \frac{P_{\text{tot}} e^{-\frac{(r-\bar{R})^2}{s}}}{n\delta g(\pi s^2 e^{-\frac{R}{s}} + \pi^{3/2} s \bar{R} (\text{erf}(\frac{\bar{R}}{s}) + 1))}} \quad (45)$$

In this case the highest temperature will occur at  $r = \bar{R}$ .

$$T(\bar{R}, \infty) = \sqrt[4]{T_{\text{sur}}^4 + \frac{P_{\text{tot}}}{n\delta g(\pi s^2 e^{-\frac{\bar{R}}{s}} + \pi^{3/2} s \bar{R} [\text{erf}(\frac{\bar{R}}{s}) + 1])}} \quad (46)$$

Numerical calculations showed that  $T_{\text{max}} < T(\bar{R}, \infty) < T(0, \infty)$  holds for all investigated cases, as can intuitively be understood from the fact that the maximal intensity for a given beam is less for a double-Gaussian shape than for a Gaussian shape, but larger than for a uniform beam.

#### 4.1.4. Calculation of the maximum temperature

Determination of the maximum temperature when radiation cooling dominated is a worst-case calculation, as there always will be some conduction cooling and often even some convection cooling. The result is presented as a nomogram, see Fig. 3, from which  $T_{\text{max}}$  can be estimated for various foil-thicknesses, ions, foil materials, foil diameters, beam shapes, beam current, and duty-cycles, with the assumption of 7.5 MeV/amu initial beam energy and a 40-Hz repetition rate. It should be observed that the evaporation rate at reduced pressure, rather than the melting point, limits the highest temperature at which the foils can be operated in vacuum. As the variation of  $T_{\text{max}}$  with the duty cycle is moderate, only 0.63% and 100% duty-cycle is shown in Fig. 3, and all other values fall in between these limits.

#### 4.2. Conduction Cooling Dominates

The equation for heat conduction in a thin circular disc is, expressed in polar coordinates with constant  $\lambda$ ,<sup>5</sup>

$$\frac{d^2 T(r, t)}{dr^2} + \frac{1}{r} \frac{dT(r, t)}{dr} - \frac{\rho C_p}{\lambda} \frac{dT(r, t)}{dt} + \frac{P_{\text{beam}}}{\lambda dl} = 0, \quad (47)$$

where  $dl$  is the thickness of the foil and  $P_{\text{beam}}$  is any beam-shape function.

#### 4.2.1. Uniform beam shape

The introduction of the uniform beam shape, as given by Eq.(13), into Eq. (47) gives

$$\frac{d^2 T(r,t)}{dr^2} + \frac{1}{r} \frac{dT(r,t)}{dr} - \frac{\rho C_p}{\lambda} \frac{dT(r,t)}{dt} + \frac{P_{tot}}{\pi R^2 \lambda dl} = 0. \quad (48)$$

The steady-state solution,  $T(r, \infty)$ , is obtained by setting the time derivative to zero and solving the resulting differential equation with the boundary conditions  $dT(0, \infty)/dr = 0$  and  $T(a, \infty) = T_{sur}$ . Assuming  $\lambda$  to be constant, the solution is then

$$T(r, \infty) = T_{sur} + \frac{P_{tot}}{4\pi \lambda dl} \left[ 1 - \left(\frac{r}{R}\right)^2 \right], \quad (49)$$

where  $R$  is the radius of the foil and  $T_{sur}$  is the temperature at the cooled edge. It is evident from Eq. (49) that the temperature of a foil of given thickness is not dependent on the size of the foil. This is easily understood as the nearest distance from a point on the foil to the edge increases linearly with  $R$  and at the same time the cross section increases linearly with  $R$ . These two effects compensate each other, which makes the temperature independent of the absolute size.

As often high and low temperatures occur on the same foil, the heat conductivity cannot be assumed to be constant. The most common approximation for  $\lambda(T)$  is Eq. (6), where  $a, b,$  and  $c$  are constants obtained by fitting Eq. (6) to experimental data.

When the heat conductivity varies it must be included in the second derivative of  $T$ . This gives Eq. (48) the following form:<sup>5</sup>

$$\frac{1}{r} \frac{\partial}{\partial r} \left\{ \lambda [T(r,t)] r \frac{\partial T(r,t)}{\partial r} \right\} - \rho C_p \frac{\partial T(r,t)}{\partial t} + \frac{P_{tot}}{\pi R^2 dl} = 0. \quad (50)$$

Introduction of Eq. (6) into Eq. (50) and taking the partial derivatives as indicated yields

$$\begin{aligned} \frac{\partial^2 T(r,t)}{\partial r^2} + \frac{1}{r} \frac{\partial T(r,t)}{\partial r} - \frac{b+2cT(r,t)^{-3}}{a-bT(r,t)+cT(r,t)^2} \left[ \frac{\partial T(r,t)}{\partial r} \right]^2 \\ - \rho C_p \frac{\partial T(r,t)}{\partial t} + \frac{P_{tot}}{\pi R^2 dl} = 0. \end{aligned} \quad (51)$$

The solution at 100% duty cycle and long times is obtained by setting the time derivative to zero in Eq. (51). The resulting differential equation was solved with a fourth-order Runge-Kutta method. The result is shown in Fig. 4 as a nomograph for Al, Be, and C foils. As can be expected from Eq. (49), the temperature in the center of the foil is independent of the radius of the foil. This was tested by integrating Eq. (51) to various radii. The results showed that the temperature at the center was independent of R.

When a pulsed beam is used the solution to Eq. (48) during the first beam pulse is

$$T(r,t) = T_{\text{sur}} + \frac{100 P_{\text{tot}}}{4\pi\lambda d l C} \left[ 1 - \left(\frac{r}{R}\right)^2 \right] - \frac{200 P_{\text{tot}}}{4\pi d l C} \sum_{n=1}^{\infty} e^{-\frac{\beta_n^2 \lambda}{R^2 \rho C_p} t} \cdot \frac{J_0\left(\frac{r}{R} \cdot \beta_n\right)}{\beta_n^3 J_1(\beta_n)} \quad (52)$$

where  $J_0$  and  $J_1$  are Bessel functions and  $\beta_n$  are the roots of the equation  $J_0(\beta_n) = 0$ . The highest temperature will as usual occur at the center of the foil. Equation (52) can then be somewhat simplified as some r terms disappear:

$$T_{\text{max}} = T_{\text{sur}} + \frac{100 P_{\text{tot}}}{4\pi\lambda d l C} - \frac{200 P_{\text{tot}}}{\pi\lambda d l C} \sum_{n=1}^{\infty} e^{-\frac{\beta_n^2 \lambda}{R^2 \rho C_p} t_{\text{on}}} \frac{1}{\beta_n^3 J_1(\beta_n)} \quad (53)$$

Equation (53) shows that the time constant for the heating cycle is determined by  $\lambda/(R^2 \rho C_p)$ . Thus a smaller foil tends to follow the variations in the beam to a larger extent than a bigger foil. Taking only the first term in the sum in Eq. (53) into account and using  $C/100 f$  for  $t_{\text{on}}$ , we obtain

$$T_{\text{max}} \approx T_{\text{sur}} + \frac{100 P_{\text{tot}}}{4\pi\lambda d l C} \left( 1 - e^{-\frac{5.783 \lambda C}{R^2 \rho C_p 100 f}} \right) \quad (54)$$

When  $100 f R^2 \rho C_p / \lambda$  is smaller than 1.25 times C, the foil will already reach its final maximum temperature during the first cycle. This condition has been used to obtain the worst-case temperatures for pulsed beam given in Fig. 4. For larger diameters the value of  $T_{\text{max}}$  will approach  $T_{\text{max}}$  for C = 100%. When the beam intensity varies with time only, the following solution to Eq. (47) is obtained, using Laplace transforms and the "faltung" theorem<sup>5,6</sup>

$$T(r, t) = T_{\text{sur}} + \frac{2\lambda}{\rho C_p R} \int_0^t Q(\tau) \sum_{n=1}^{\infty} e^{-\frac{\lambda \beta_n^2 (t - \tau)}{\rho C_p}} \cdot \frac{J_0(r \beta_n)}{a_n J_1(R \beta_n)} d\tau, \quad (55)$$

where  $Q(\tau)$  is the beam intensity as a function of time and  $\beta_n$  are the roots to the Eq.  $J_0(\beta_n) = 0$ .

When the beam is pulsed [Eqs. (17a) and (17b)] the integrand is zero during the "off" part of the beam cycle and  $Q(\tau)$  is constant during the "on" part of the beam cycle. Thus the integral in Eq. (55) can be replaced by a sum giving the solution

$$T(r, t) = T_{\text{sur}} + \frac{200 P_{\text{tot}}}{\pi C \lambda d l} \sum_{n=1}^{\infty} \frac{J_0\left(\frac{r}{R} \beta_n\right)}{\beta_n^3 J_1(\beta_n)} \left\{ e^{-\frac{\beta_n^2 \lambda t}{\rho C_p R^2}} \left( e^{\frac{\beta_n^2 C \lambda}{100 \rho C_p f R^2}} - 1 \right) \sum_{m=0}^M e^{-\frac{\beta_n^2 \lambda m}{\rho C_p f R^2}} + \delta \left[ 1 - e^{-\frac{\beta_n^2 \lambda}{\rho C_p R^2} \left( t - \frac{M+1}{f} \right)} \right] \right\}, \quad (56)$$

where  $\beta_n$  is the solutions to the equation  $J_0(\beta_n) = 0$ ,  $M$  is the integer number of complete beam cycles contained within  $t - (C/100 f)$ ,  $\delta$  is a delta function which has the value 0 when  $t$  corresponds to the beam-off part and the value 1 when  $t$  corresponds to the beam-on part of the beam cycle. Equation (56) transforms to Eq. (53) for the first beam pulse ( $M=0$ ,  $\delta=0$ ) and to Eq. (49) for  $C = 100$ .

It is seen from Eq. (56) that the cooling-off time constants are  $\beta_n^2 \lambda / \rho C_p R^2$  and the same as the heating time constants. Figure 5 shows the central temperature as a function of time for some values of  $C$  when the time constant is comparable to the frequency. It is obvious that the large increase in  $\lambda$  obtained by cooling the edge to low temperatures will result in more rapid (and larger) temperature fluctuations. The increase in  $\lambda$  can to some degree be compensated by increasing the foil diameter, but this leads easily to such large diameters that the beam shape no longer is uniform. The increase in  $\lambda$  can also be compensated by using a higher frequency. The effect of foil diameter on the center temperature is shown in Fig. 6.

#### 4.2.2. Gaussian beam shape

When the beam has any non-uniform shape,  $p_{\text{beam}}$  in Eq. (47) will be dependent on  $r$ . In the case of a Gaussian beam shape we obtain

$$\frac{d^2 T(r, t)}{dr^2} + \frac{1}{r} \frac{dT(r, t)}{dr} - \frac{\rho C_p}{\lambda} \frac{dT(r, t)}{dt} - \frac{P_{\text{tot}} \ln(1-\alpha)}{\pi R_a^2 \lambda d l} e^{-\left(\frac{r}{R_a}\right)^2 \sqrt{-\ln(1-\alpha)}} = 0. \quad (57)$$

The steady-state solution,  $T(r, \infty)$ , is obtained by setting the time derivative to zero and solving the resulting differential equation with the boundary conditions  $dT(0, \infty)/dr = 0$  and  $T(R, \infty) = T_{\text{sur}}$ . Assuming  $\lambda$  to be constant, the solution is

$$T(r, \infty) = T_{\text{sur}} + \frac{P_{\text{tot}} \sqrt{-\ln(1-\alpha)}}{4\pi\lambda d l} \sum_{n=1}^{\infty} (-1)^{n-1} \frac{[-\ln(1-\alpha)]^{n/2} \left[1 - \left(\frac{r}{R}\right)\right]^n}{n \cdot n!}, \quad (58)$$

where  $\alpha$  is the fraction of the total beam current hitting the foil and  $P_{\text{tot}}$  is the total power released by the beam. As usual, the highest temperature will occur at the center of the foil ( $r = 0$ ). By introducing  $r = 0$  in Eq. (58) we obtain the equation for  $T_{\text{max}}$ ,

$$T_{\text{max}} = T_{\text{sur}} + \frac{P_{\text{tot}} \sqrt{-\ln(1-\alpha)}}{4\pi\lambda d l} \sum_{n=1}^{\infty} (-1)^{n-1} \frac{[-\ln(1-\alpha)]^{n/2}}{n \cdot n!}, \quad (59)$$

which is very similar to Eq. (49) with  $r = 0$ . Figure 7 shows the shape factor  $\psi(\alpha)$  as a function of the transmission factor  $\alpha$ .

$$\psi(\alpha) = \sqrt{-\ln(1-\alpha)} \sum_{n=1}^{\infty} (-1)^{n-1} \frac{[-\ln(1-\alpha)]^{n/2}}{n \cdot n!}. \quad (60)$$

Using  $\psi$ , equation (59) can be written as

$$T_{\text{max}} = T_{\text{sur}} + \frac{P_{\text{tot}}}{4\pi\lambda d l} \cdot \psi(\alpha). \quad (61)$$

If the transmitted beam power is used instead of the total beam power, Eq. (61) changes to

$$T_{\text{max}} = T_{\text{sur}} + \frac{P_{\text{tr}}}{4\pi\lambda d l} \cdot \frac{\psi(\alpha)}{\alpha}. \quad (62)$$

The function  $\psi(\alpha)/\alpha$  vs  $\alpha$  is shown in Fig. 8. A comparison of Figs. 2 and 8 shows that the temperature rises more rapidly with  $\alpha$  for conduction cooling than for radiation cooling.

The complete time-dependent solution of Eq. (57) was not obtained because of difficulties with the solution of the new differential equation obtained after Laplace transformation of Eq. (57). An analytical solution for a pulsed Gaussian beam was not obtained for the same reasons. A numerical solution is shown in Fig. 10.

#### 4.2.3. Favorable beam shapes

The uniform beam can be regarded as one in a series of simple  $r$ -dependent beam shapes of the general type

$$p_{\text{beam}} = k \cdot r^n, \quad (63)$$

where the uniform beam corresponds to  $n = 0$ . The total beam power is then given by

$$P_{\text{tot}} = \int_0^R 2\pi k r^{n+1} dr, \quad (64)$$

from which  $k$  can be determined:

$$k = \frac{(n+2) P_{\text{tot}}}{2\pi R^{n+2}}, \quad (65)$$

The steady-state solution of the heat-conduction equation is then

$$T(r, \infty) = T_0 + \frac{P_{\text{tot}}}{2(n+2)\pi\lambda dl} \left[ 1 - \left(\frac{r}{R}\right)^{2+n} \right], \quad (66)$$

where  $n = 0, 1, 2, 3$  etc.

It can be seen from Eq. (66) that the maximum temperature decreases as  $n$  increases. When  $T_0$  can be neglected, the following relations are obtained between the temperatures:

$$T_{\text{max}}(n) = \frac{2}{2+n} T_{\text{max}}(\text{even-beam}). \quad (67)$$

And thus lower temperature can be obtained by choosing a beam shape which corresponds to a higher value of  $n$  in Eq. (63), i.e., by concentrating the beam to a small area near the rim.

### 4.3. Convection-Cooling Dominates

When convection cooling dominates over radiation cooling and conduction cooling, the amount of heat generated by the beam is equal to the amount of heat carried away by convection from any point on the foil. Thus we obtain the relation (one-sided cooling)

$$P_{\text{beam}} = h [ T(r, t) - T_{\text{fluid}} ] + \rho C_p dl \frac{dT(r, t)}{dt}, \quad (68)$$

where  $h$  is a function of  $T(r, t)$ ,  $T_{\text{fluid}}$ ,  $w$ , etc., as given by Eqs. (8), (9), (10), or (11). The resistance to heat flow through the thin foil is neglected.  $T_{\text{fluid}}$  can be calculated with sufficient accuracy from  $P_{\text{tot}}$ ,  $w$ ,  $(C_p)_{\text{fluid}}$ , and the entrance temperature of the fluid,  $T_{\text{fluid}}^0$ :

$$T_{\text{fluid}} \approx T_{\text{fluid}}^0 + \frac{P_{\text{tot}}}{w (C_p)_{\text{fluid}}}, \quad (69)$$

where  $P_{\text{tot}}$  is the total beam power released in the foil and fluid. Analytic solutions to Eq. (68) can usually not be obtained because  $h$  is often given by a function containing fractional powers of  $T(r, t)$ . The stationary state at constant beam can, however, be expressed analytically in some cases.

#### 4.3.1. Water cooling

In the case of laminar flow of water,  $h$  is given by Eq. (9). For a uniform beam shape the temperature is almost constant on the foil and is given by the equation

$$T(r, \infty) = \sqrt[3]{ \left\{ \frac{P_{\text{tot}} \cdot 10^4}{\pi R^2 (2.685 T_w + 51.62)} \right\}^4 } + T_w, \quad (70)$$

where  $T_w$  is the water mean temperature. At sufficiently large flow rates  $T_w \approx T_w^0$ , where  $T_w^0$  is the temperature of the incoming water. As can be seen from Eq. (70), the foil temperature is independent of  $r$ . The temperature increases roughly with the 1.33 power of  $P_{\text{tot}}$  and decreases roughly with the 2.66 power of  $R$ .

When the beam shape is Gaussian the temperature is given instead by



$$T(r, \infty) = e^{-\frac{r^2}{R_a^2} \cdot \frac{4}{3} \sqrt{-\ln(1-a)}} \sqrt[3]{\frac{-P_{\text{tot}} \ln(1-a) \cdot 10^4}{\pi R_a^2 (2.685 T_w + 51.62)}}^4 + T_w \quad (71)$$

and  $T(r, \infty)$  varies with radius like  $a \cdot e^{-br^2} + c$ , i. e., in the same manner as the beam shape.

The water cooling is very effective in comparison with radiation cooling or conduction cooling. At a mean water temperature of 300° K,  $P_{\text{tot}}/\pi R^2 \approx 3.8$  (kW/cm<sup>2</sup>) is needed to increase the foil temperature to 373° K. In comparison, a foil temperature of 373° K at pure radiation-cooling is reached for  $P_{\text{tot}}/\pi R^2 \leq 0.13$  (W/cm<sup>2</sup>). Conduction cooling is more difficult to compare with, as it varies with  $P_{\text{tot}}/dl$  instead of  $P_{\text{tot}}/\pi R^2$ , but it is usually intermediate in efficiency. At a water temperature of 20° C and a surface temperature of 100° C the heat resistance at the metal-water interface corresponds to 84 cm copper.

#### 4.3.2. Gas cooling

The heat-carrying capacity of gases is less than for water. Hence it is necessary to use large flow rates to obtain a good cooling with gases. When turbulent flow exists, Eq. (10) can be used to calculate the film coefficient,  $h$ . Then the foil temperature at uniform beam shape is given by

$$T(r, \infty) = T_g^0 + \frac{P_{\text{tot}} + P_g}{w(C_p)_g} + \frac{P_{\text{tot}}}{\pi R^2} \cdot \frac{D}{0.023 \lambda_g} \cdot \left(\frac{DV\rho_g}{\mu}\right)^{-0.8} \left(\frac{(C_p)_g \mu}{\lambda_g}\right)^{-0.4}, \quad (72)$$

where subscript  $g$  refers to the gas,  $V$  is the linear gas velocity (cm/sec),  $D$  is the diameter of the gas channel, and  $w$  is the gas flow rate (g/sec). It can be seen that the foil temperature is very nearly inversely proportional to the gas flow rate. The term  $P_g$  accounts for the heat generated in the gas during passage of the cooling channel.

## 5. NUMERICAL SOLUTION OF THE GENERAL CASE

In practice, the observed beam functions and foil arrangements often deviate from the simple shapes and forms discussed above. It is then necessary to solve Eq. (33) numerically for arbitrary beam shapes, foil geometries, and cooling arrangements. At the same time it is necessary to use temperature-dependent heat conductivities and heat capacities to make a realistic calculation.

A program was thus developed where the only assumptions are: beam-power is independent of temperature, radiation can only escape in the  $l$ -direction, convection cooling is only possible in the  $x$ - $y$  plane, the grayness factors are temperature-independent, and  $\lambda$  and  $C_p$  values can be expressed with sufficient accuracy as second-degree polynomials in  $T$ .

A mesh system is set up in the  $x$ - $y$  plane which is then reproduced as layers in the  $l$  direction. At each mesh-point, the beam power, starting temperature, grayness factor, geometrical connection to adjacent points in the positive coordinate directions, type of polynomials for  $\lambda$  and  $C_p$ , and type of point—i. e., internal or boundary—is specified. The mesh width is prescribed for each coordinate separately.

Starting at a corner and proceeding through the whole mesh system, excluding boundary points, the temperature-heat conductivity product is interpolated from the surrounding mesh points by using a second-degree interpolation formula. This results in almost as many linear equations as there are mesh-points. The large number of mesh-points desirable makes normal solution by matrix-inversion impractical. Therefore the Gauss-Siedel iteration method was employed, as then only one equation had to be evaluated at a time. The coefficients were recalculated every time, thus avoiding the storage of large sparse matrices, of the size of about 250 000 elements. The Gauss-Siedel iteration is convergent, as the main diagonal elements are larger than the other elements in each row and the matrix is positive definite.<sup>6</sup>

The power lost by radiation and convection is calculated from the new set of temperatures in the mesh-points and subtracted from the power released from the beam. Then the whole iteration cycle is repeated until a new iteration changes all temperatures with less than a prescribed value.

The calculation can be performed to obtain a steady-state solution by setting all  $C_p$  values to zero or to obtain snapshots at given time intervals with a continuous or pulsed beam.

Symmetry axes can be used freely to reduce the problem as long as the  $\lambda$  values,  $C_p$  values, and grayness factors for mesh-points at a symmetry cut are divided by the appropriate number of used symmetry axes passing through the mesh-point. Values beyond a symmetry axis will then be mirror images of the values before the axis.

For very thin foils, the heat conduction in the  $l$  direction is much larger than in the  $x$  and  $y$  directions. This may cause numerical difficulties which can give a premature halt in the calculations. The simplest cure is to treat such foils as 2-dimensional structures, which is equivalent to neglecting the resistance to heat flow in the  $l$  direction as compared to the resistances in the  $x$ - $y$  plane. The heat conductivity and heat capacity are automatically multiplied by the actual thickness in a 2-dimensional treatment and by the product of thickness and length in a 1-dimensional case.

For cases where the beam power is small compared to the heat-capacity, it may be necessary to decrease the value of the allowed difference between two successive iterations. On the other hand, high values for the grayness factors seems to increase the convergence rate.

A complete listing of the program is given in Appendix 2. Appendix 3 gives a sample of input data and results. The organization and format of the input data is shown in Appendix 1. The algorithm is slightly modified, as the number of subscripts must be limited to three to be able to use the Fortran compilers available for the CDC-6600 and CDC-7600 computers. This is the reason for the split of the temperature array into two arrays (T and TG) and of the coupling-constant array into three arrays (CX, CY, and CZ) etc.

#### 5.1. Combined Radiation and Conduction Cooling

The variation of temperature with radius and time can be obtained for any given foil, foil-material, ion, beam-shape, frequency, duty-cycle, and mean current with the aid of the program given in Appendix 2. To illustrate the effect of beam-pulsing and beam shape on foil temperature, a half-mil-thick gold foil of 1 cm diameter was chosen. The edge of the foil is clamped to 20° C and the surroundings are assumed to be at 20° C. The foil is surrounded on both sides by vacuum. The ion chosen was  $^{40}\text{Ar}^{13+}$  of

7.2 MeV/amu, which is typical for an Ar beam from the Berkeley SuperHILAC. These ions will release  $10.9 \text{ W}/\mu\text{A}$  ( $^{40}\text{Ar}^{13+}$ ) during their passage through a half-mil gold foil.

Figure 9 shows the variation of temperature with radius and time for an incident beam with a uniform shape. The steep increase of temperature near the edge of the foil is typical for the uniform beam shape. Figure 10 shows the variation of temperature with radius and time for a Gaussian beam shape. Here the temperature increases more rapidly towards the center, leading to higher maximum temperature. Figure 11 shows the effect of a double-Gaussian beam shape. Typical for this case is the delayed heating of the central part of the foil, leading to a lower maximum temperature than for a simple Gaussian beam shape.

When the foil thickness is decreased, the differential energy-loss ( $dE/dl$ ) of the beam becomes constant. For very thin foils the equilibrium temperature is determined by the radiation cooling, and the foil temperature falls approximately with the fourth root of the thickness,  $l$ , [see Eq. (36)], as  $P_{\text{tot}}$  is a linear function of  $l$ . For thicker foils, where  $dE/dl$  still is constant, the temperature becomes independent of the foil thickness, as the cooling is mainly by conduction. In this case both the beam power and the conduction area vary linearly with the thickness [see Eq. (47)]. When the foil thickness approaches the range of the ions in the foil material,  $dE/dl$  increases, which leads to an increase in the foil temperature with thickness. When the foil is thicker than the range of the ions, the temperature drops again with increasing thickness—almost linearly at first, as long as the thickness is small compared to the diameter, and then the temperature levels off to a constant value, determined by conduction in the  $l$  direction. This temperature is mainly independent of the type of ion and depends almost only on the energy per charge unit, the beam current, and the foil diameter.

#### ACKNOWLEDGMENT

The author is indebted to Prof. G. T. Seaborg, Drs. J. Alonso, A. Ghiorso, J. Kratz, and M. Nurmi for encouraging and helpful discussions, and to the Swedish Atomic Research Council for economic support.

This work was done under the auspices of the U. S. Atomic Energy Commission.

References

1. Northcliffe and Schilling, Range and Stopping-Power Tables for Heavy Ions, p. 252, Nuclear Data Tables.
2. F. W. Hutchinson, Industrial Heat Transfer (Industrial press, New York, 1952).
3. F. Nichel and H. Ewald, Überlegungen über Temperaturverhalten und Lebensdauer von dünnen Targets im gepulsten Schwerionenstrahl, Internal report GSI.
4. H. Prange, Targetfragen beim Experimentieren mit intensiven Strahlen Schweren Ionen, p. 1, GSI-Bericht 72-10, Gesellschaft für Schwerionenforschung mbH, Darmstadt, 1972.
5. H. S. Carslaw and S. C. Jaeger, Conduction of Heat in Solids (Clarendon Press, Oxford, 1959).
6. G. A. Korn and T. M. Korn, Mathematical Handbook for Scientists and Engineers, 2<sup>nd</sup> ed. (McGraw-Hill, New York, 1968).
7. R. L. Weber, Heat and Temperature Measurement (Prentice-Hall, New York, 1950).
8. G. V. Samsonov, Editor, Handbook of the Physicochemical Properties of the Elements (IFI/Plenum, New York, 1968).

Appendix 1.

Input data for HEAT v4m1

(Always punch the decimal point!)

1. HEADING-CARD (15A4)

Column 1 to 60: Alphanumeric text, which will be used as a heading on printout.

2. BEAM-CARD (8F10.0)

(A blank BEAM-CARD defines END-OF-DATA.)

- 2.1 Beam-Current in  $\mu\text{A}$ . Normally as mean particle current.
- 2.2 Beam-Energy-loss in MeV/Grid-unit. (See Grid-point cards!)
- 2.3 Beam-pulse on-time in seconds. (Only for pulsed beam, else 1.0)
- 2.4 Beam-pulse off-time in seconds. (Only for pulsed beam, else 0.0)
- 2.5 Melting temperature in  $^{\circ}\text{C}$ . (Default is 10 000  $^{\circ}\text{C}$ . Melted material is removed)
- 2.6 Temperature offset in  $^{\circ}\text{C}$ . (The offset is added to all grid-point-temperatures before calculation).
- 2.7 Surrounding radiation temperature in  $^{\circ}\text{C}$ . (Default is -273.16  $^{\circ}\text{C}$ )
- 2.8 Grayness factor (Default is 1.0)

3. GRID-DIMENSION-CARD (8F10.0)

- 3.1 Grid-spacing, X-direction, in cm.
- 3.2 Grid-spacing, Y-direction, in cm.
- 3.3 Grid-spacing, Z-direction, in cm. (Z is parallel to the beam)
- 3.4 Grid-spacing, time-direction, in seconds. (Zero implies a steady-state condition)
- 3.5 Time before full printout, in seconds. (Neglected for steady state)
- 3.6 Time when calculation stops, in seconds. (Neglected for steady state)

4. COOLING-TYPE-CARD (I5)

- 4.1 COOLING TYPE  $\left\{ \begin{array}{l} 0=\text{VACUUM ON BOTH SIDES IN } x\text{-}y \text{ plane} \\ 1=\text{GAS FLOWS ON ONE SIDE, PARALLEL} \\ \text{TO THE } x\text{-}y \text{ plane.} \end{array} \right.$

5. GAS-DATA-CARDS (8F10.0)

(Only when cooling-type is 1)

5.1 Hydraulic diameter of cooling channel, in cm.

5.2 Heat conductivity of gas expressed as a Sutherland approximation

( $\lambda_{\text{gas}} = a T \sqrt{T} / (b + T)$ , with T in °K), in W/cm degree.

5.2.1 a.

5.2.2 b.

5.3 Viscosity of gas expressed as a Sutherland approximation.

( $\mu_{\text{gas}} = a T \sqrt{T} / (b + T)$ , with T in °K), in poise.

5.3.1 a.

5.3.2 b.

5.4 Heat capacity of gas expressed as a polynomial

( $C_{p\text{gas}} = a + bT + c/T^2$ , with T in °K), in J/g, degree.

5.4.1 a.

5.4.2 b.

5.4.3 c.

5.5 Volume expansion coefficient of gas.

5.6 Flow-rate of gas, in g/sec.

5.7 Entering temperature of gas, in °C.

5.8 Gas pressure in atm.

5.9 Molecular weight of gas.

(The gas-cooling utilizes several similarity rules and rough approximations, hence the result should not be regarded as very accurate!)

6.  $\lambda_x$ -NUMBER CARD (15)

6.1 Number of heat-conductivities. ( $\leq 10, \geq 1$ )

7.  $\lambda_x$ -FUNCTION-CARDS (3F10.0)

One card for each heat-conductivity type. The heat conductivity is expressed as  $\lambda_x = a + bT + c/T^2$ , where T is in °K and  $\lambda_x$  in W/cm degree.

7.1 a.

7.2 b.

7.3 c.

The first card will be type 1, the 2<sup>nd</sup> type 2, etc. See 15.

8.  $\lambda_y$ -NUMBER CARD (I5)

8.1 Number of heat conductivities. ( $\leq 10, \geq 1$ )

For a one-dimensional case, only one dummy  $\lambda_y$  is needed.

9.  $\lambda_y$ -FUNCTION CARDS (3F10.0)

Same as 7, but for conduction in y-direction.

10.  $\lambda_z$ -NUMBER CARD (I5)

10.1 Number of heat-conductivities. ( $\leq 10, \geq 1$ ).

For a one- or two-dimensional case, only one dummy  $\lambda_z$  is needed.

11.  $\lambda_z$ -FUNCTION CARDS (3F10.0)

Same as 7, but for conduction in z direction.

12.  $C_p$ -NUMBER CARD (I5)

12.1 Number of  $C_p$ -types ( $\geq 1, \leq 10$ ).



13. C<sub>p</sub>-FUNCTION CARD (3F10.0)

One card for each C<sub>p</sub> type. First card will be type 1, second type 2, etc.

C<sub>p</sub> is expressed as a polynomial  $C_p = a + bT + c/T^2$ , where T is in °K and C<sub>p</sub> in J/ml degree. (OBS! not J/g degree)

13.1 a.

13.2 b.

13.3 c.

14. GRID-NUMBER CARD (3I5)

14.1 Number of grid lines crossing x coordinate ( $\geq 1, \leq 10$ )

14.2 Number of grid lines crossing y coordinate ( $\geq 1, \leq 10$ )

14.3 Number of grid lines crossing z coordinate ( $\geq 1, \leq 5$ )

15. GRID-POINT CARDS (6I3, 2X, 6F10.0)

Grid-point cards are needed to specify points deviating from the default assumption: outside beam area, clamped at 0°C and without connection to surrounding points. (A point is the crossing of three grid lines). One card per grid point.

15.1 Number of grid lines from origin along x axis. ( $> 0. \leq 10$ )

15.2 Number of grid lines from origin along y axis. ( $> 0. \leq 10$ )

15.3 Number of grid lines from origin along z axis. ( $> 0. \leq 5$ )

A card with 0 grid-lines from origin terminates the reading of grid-point cards. Normally grid-line no. 1 goes through origin.

15.4 C<sub>p</sub>-function type for this point ( $\geq 1, \leq 10$ )

15.5  $\lambda$ -function type for this point ( $\geq 1, \leq 10$ )

The type selected is common for  $\lambda_x, \lambda_y,$  and  $\lambda_z$ . The  $\lambda_x$  is considered

to be for conduction between this point and the next along the  $x$  axis. The same holds for  $\lambda_y$  and  $\lambda_z$ .

15.6 Gas contact. (0 = no gas contact, 1 = gas contact.)

15.7 Temperature in degrees centigrade. (Starting value includes temp. offset.)

15.8 Fraction of beam power released at the point. (Beam power-loss must be normalized to this value.)

15.9 Point type. 1.0 means that temperature is clamped to its initial value. 0.0 means that no radiation is lost from this point. When heat radiation can escape in the  $z$  direction,  $-G$  is specified, where  $G$  is the surface grayness factor  $0 < G < 1.0$ . For 2-dimensional foils  $G$  is the sum of the grayness factors for both surfaces.

15.10 Fractional area coupling to next point in  $x$  direction.

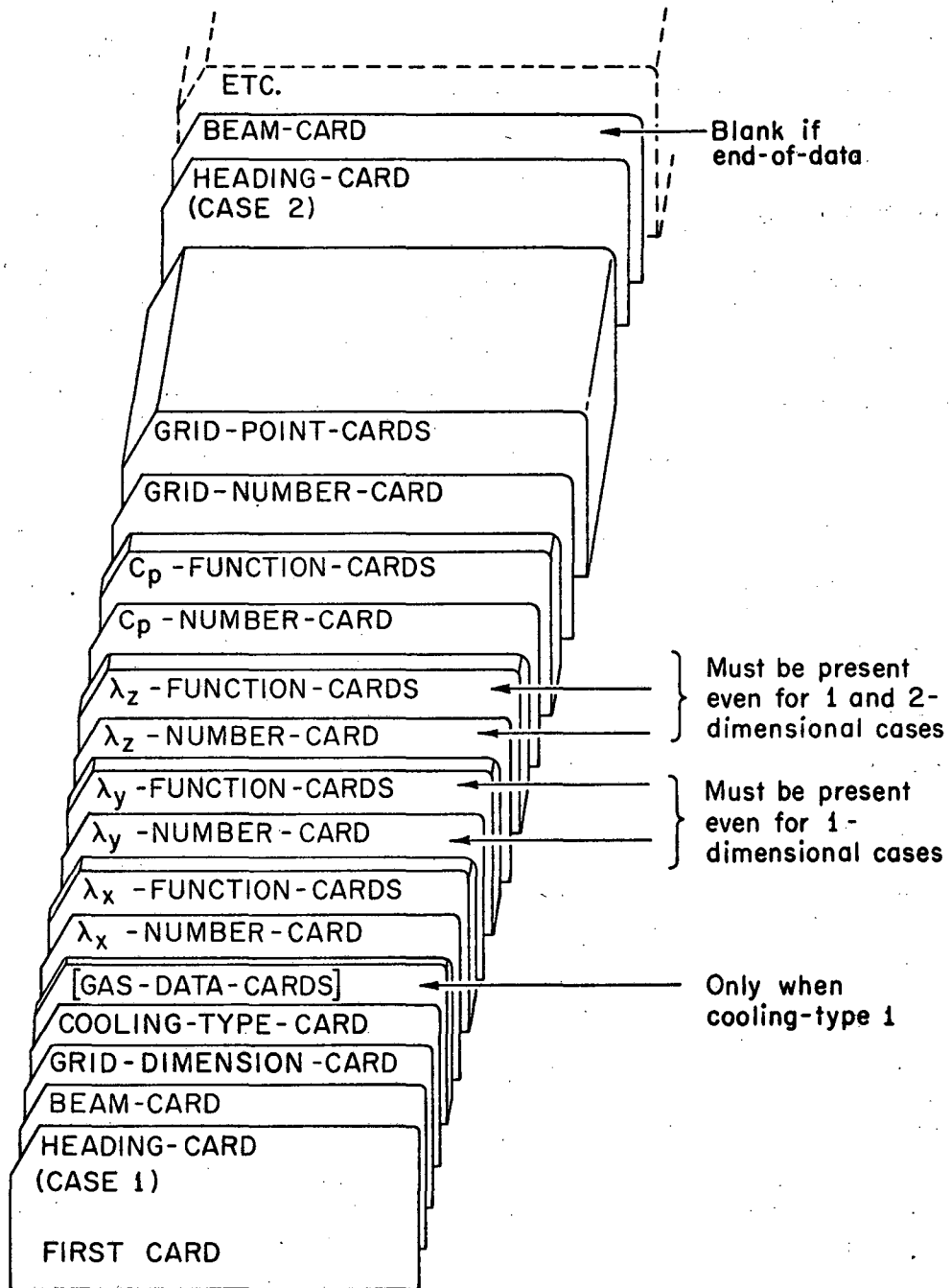
15.11 Fractional area coupling to next point in  $y$  direction.

15.12 Fractional area coupling to next point in  $z$  direction.

The fractional areas are especially useful when symmetry properties are used to reduce the size of a problem.

The test example supplied with the program is for 1 quadrant of an approximately circular foil with no radiation or gas cooling. It shows that the coupling areas (15.10 - 15.12) are not reduced along the symmetry axes, but how instead three different  $\lambda$  and  $C_p$  sets are used and the fractional beam (15.8) is used to adjust the conditions along the symmetry lines. Thus functions and coupling areas can be traded against each other to simplify a problem.

Arrangement of data-deck for HEAT v4m1



APPENDIX 2. Program HEAT v4m1

HEAT

PROGRAM HEAT(INPUT,OUTPUT,TAPE5=INPUT,TAPE6=OUTPUT)

C  
C PROGRAM FOR SOLVING DYNAMIC AND STATIC 3-D HEAT-TRANSFER WITH  
C POWER-SOURCES, RADIATION COOLING, HEAT-CONDUCTION IN NONISOTROPIC  
C CASES. RADIATION SOURCES ARE TREATED AS BLACK BODIES. HEAT-TRANS  
C FER COEFFICIENTS AND HEAT-CAPACITIES CAN BE LINEARLY DEPENDENT ON  
C TEMPERATURE. THE POWER SOURCES MAY BE IN TWO STATES FOR GIVEN  
C TIME INTERVALS.  
C  
C J.O.LILJENZIN 29.9.1972  
C  
C VERSION 4 USES POLYNOMIALS  $A+B*T+C/T**2$  FOR HEAT-CONDUCTIVITIES  
C TO ALLOW A LARGER TEMPERATURE RANGE TO BE COVERED  
C WHEN THIS IS NOT NECESSARY, USE V3M0 WHICH IS FASTER.  
C  
C UA=BEAM CURRENT IN UA(DC)  
C PA=BEAM-POWER LOST IN MEV/POINT  
C TON=TIME INTERVAL WITH BEAM ON  
C TOFF=TIME-INTERVAL WITH BEAM OFF  
C UA.LE.0. STOPS PROGRAM  
C DX=CM/GRID-UNIT IN X-DIRECTION  
C DY=CM/GRID-UNIT IN Y-DIRECTION  
C DZ=CM/GRID-UNIT IN Z-DIRECTION  
C DT=TIME-STEP IN SECONDS  
C IF DT=0. THE STEADY-STATE IS CALCULATED  
C TMAX=TIME-LIMIT IN SECONDS (STOPS THE PRESENT CASE)  
C TMIN IS THE RUN-IN TIME BEFORE FIRST COMPLETE PRINT-OUT  
C MX=TOTAL NO. OF RX-FUNCTIONS  
C AX(I) AND BX(I) ARE THE COEFFICIENTS IN THE EXPRESSION  
C  $RX(I,J,K)=CX(I,J,K)*(AX(L)+BX(L)*T(I,J,K))*XM$  (WHERE  $L=NR(I,J,K)$ )  
C THE AX(I).S ARE IN W/CM DEG. AT 0 DEG.K (NOT DEG C)  
C THE BX IS IN W/CM(DEG)\*\*2  
C MY, AY(I) AND BY(I) ARE THE SAME FOR RY  
C MZ, AZ(I) AND BZ(I) ARE THE SAME FOR RZ  
C MC, AC(I) AND BC(I) ARE THE CORRESPONDING DATA FOR THE HEAT-  
C CAPACITY. AC(I).S IN J/MLDEG AT 0 DEG. K  
C BC.S IN J/ML(DEG)\*\*2  
C IM=NUMBER OF GRID-POINTS IN X-DIRECTION  
C JM=NUMBER OF POINTS IN Y-DIRECTION  
C KM=NUMBER OF POINTS IN Z-DIRECTION  
C LM=DIMENSIONALITY OF ACTUAL CASE  
C I=NO. OF DX TO A POINT -1  
C J=NO. OF DY TO A POINT -1  
C K=NO. OF DZ TO A POINT-1  
C T(I,J,K)=TEMPERATURE IN DEG.C AT POINT I,J,K AND TIME  
C Q(I,J,K)=FRACTION OF POWER AT POINT I,J,K  
C F(I,J,K)=1. MEANS T(I,J,K)=CONSTANT (BORDER)  
C =0. MEANS T(I,J,K)=VARIABLE  
C =-V. MEANS T(I,J,K)=VARIABLE AND RADIATION FROM V  
C SURFACES IN THE X-Y-PLANE (EACH AREA IS DY\*DX)  
C CX(I,J,K)=COUPLING-CONSTANT BETWEEN I AND I+1  
C CY(I,J,K)=DITO FOR J AND J+1  
C CZ(I,J,K)=DITO FOR K AND K+1  
C NR(I,J,K) SELECTS THE APPROPRIATE RX-, RY-, AND RZ-FUNCTIONS  
C NC(I,J,K) SELECTS THE APPROPRIATE C-FUNCTION  
C ITER IS LOOP-COUNTER

HEAT

C SUM IS CONVERGENCE-TEST AGAINST RKT  
C  
C OBSERVE THE POSSIBILITY TO UTILIZE SYMMETRIES TO REDUCE A GIVEN  
C PROBLEM.  
C WHEN SYMMETRY IS USED THE Q, C AND V.S FOR A POINT MUST BE  
C DIVIDED BY THE NUMBER OF USED SYMMETRY AXES PASSING THRU THIS  
C POINT.  
C OBSERVE ALSO THAT THE RZ-S OF A HIGHER LAYER (LARGER K) AFFECTS  
C THE RZ-S OF THE NEXT LOWER LAYER. THIS IS ALSO TRUE FOR MATERIAL  
C CHANGES IN THE X- AND Z-DIRECTIONS.  
C TSUR IS SURROUNDING TEMPERATURE TO BE USED FOR CALC OF RAD COOL  
C  
C FOR CYCLIC PHENOMENA IT IS ADVISED TO START BY OBTAINING YOUR  
C STEADY-STATE CONDITIONS AT THE MEAN-POWER USED AND THEN USE THIS  
C AS THE STARTING POINT FOR THE T(X,Y,Z,T) CALCULATIONS.  
C TADD IS ADDED TO ALL POINT-TEMPERATURES  
C  
C VERSION 3 ALLOWS GAS-COOLING ON RADIATING SURFACES  
C  
C ITYPE=0 FOR NO GAS-COOLING (=VACUUM)  
C 1 FOR GAS-COOLING  
C  
C CD IS CHARACTERISTIC DIAMETER (CM)  
C CK=GAS HEAT CONDUCTIVITY (W/CM.DEG)  
C CKA AND CKB ARE CONSTANTS IN  $CK=CKA*T^{1.5}/(T+CKB)$   
C GMU IS GAS BULK VISCOSITY  
C GMUF IS GAS VISCOSITY IN BOUNDARY LAYER  
C CMA AND CMB ARE CONSTANTS IN  $MU=CMA*T^{1.5}/(T+CMB)$   
C CP IS GAS HEAT CAPACITY (J/G DEG.)  
C CPA,CPB AND CPC ARE COEFFICIENTS IN  $CP=CPA+CPB*T+CPC/T^{**2}$   
C CB IS VOLUME EXPANSION COEFFICIENT (/DEG.)  
C CW IS GAS MASS FLOW (G/S)  
C CTC IS GAS TEMPERATURE AT INLET (DEG. C)  
C CPRES IS GAS PRESSURE AT TARGET SURFACE (ATA)  
C CMV IS THE MOLECULAR WEIGHT OF THE GAS  
C  
C CR IS GAS DENSITY (G/ML) FROM THE GAS LAW  
C CONA AND CONB ARE CONSTANTS FOR GIVEN GAS, BULK TEMP AND PRESSURE  
C GT IS CALCULATED MEAN TEMPERATURE OF GAS (DEG.K)  
C NG(I,J,K) IS 1 IF GAS IS IN CONTACT WITH THIS POINT  
C 0 IF NO GAS-CONTACT  
C QTG IS TOTAL HEAT TRANSFERRED TO GAS-PHASE  
C  
C DIMENSION F(10,10,5),T(10,10,5),TG(10,10,5),Q(10,10,5),AX(10),  
C 1BX(10),AY(10),BY(10),AZ(10),BZ(10),AC(10),BC(10),PR(10),PT(15),  
C 2CX(10,10,5),CY(10,10,5),CZ(10,10,5),DC(10),EX(10),EY(10),EZ(10),  
C 3NR(10,10,5),NC(10,10,5),NG(10,10,5)  
C  
C STATEMENT FUNCTIONS  
C SUD EVALUATES SUTHERLAND EQN AND POL POLYNOMIAL  
C  $SUD(A,B,C)=A*C^{1.5}/(B+C)$   
C  $POL(A,B,C,D)=A+B*D+C/D^{**2}$   
C  
C IVERS=4  
30 MODIF=1  
31 1000 TIME=0.

```

HEAT
32      ITER=-1
33      RKT=0.
34      DO 1 I=1,10
35      DO 1 J=1,10
36      DO 1 K=1,5
50      F(I,J,K)=1.
51      T(I,J,K)=0.
51      TG(I,J,K)=0.
52      CX(I,J,K)=0.
53      CY(I,J,K)=0.
53      CZ(I,J,K)=0.
54      NR(I,J,K)=0
54      NC(I,J,K)=0
55      NG(I,J,K)=0
55      Q(I,J,K)=0.
C
63      READ(5,4)(PT(I),I=1,15)
4       FORMAT(15A4)
70      WRITE(6,5)(PT(I),I=1,15),IVERS,MODIF
5       FORMAT(1H1,15A4,9HHEAT VERS,I3,5H MOD,I3)
C
102     READ(5,2)UA,PA,TON,TOFF,TMLT,TADD ,TSUR,GSIGE
2       FORMAT(8F10.0)
126     IF(UA.LE.0.) STOP
132     IF(TMLT.LE.0.) TMLT=10000.
135     IF(TSUR.EQ.0.) TSUR=-273.16
137     READ(5,2)DX,DY,DZ,DT,TMAX,TMIN
157     IF(DT)200,200,201
C       SET CONDITIONS FOR A STEADY-STATE CASE
161     200 TON=1.
162     TOFF=0.
163     TMAX=0.
164     201 CONTINUE
164     WRITE(6,3)UA,PA,TON,TOFF,TMLT
3       FORMAT(6H0BEAM=,F10.3,10HUA, POWER=,E10.3,9HMEV/POINT,5H TON=,
1F10.4,8HS, TOFF=,F10.4,14HS, MELTS AT T=,F10.2)
202     TMTT=TMLT+273.16
C
204     WRITE(6,6)DX,DY,DZ,DT,TMAX,TMIN
6       FORMAT(4H0DX=,F10.5,7HCM, DY=,F10.5,7HCM, DZ=,F10.5,7HCM, DT=,
1F10.5,10HSEC, TMAX=,F10.5,10HSEC, TMIN=,F10.5,3HSEC)
224     IF(TMIN.GE.TMAX.AND.DT.NE.0.) GO TO 1000
234     WRITE(6,444)TSUR
444     FORMAT(6H0TSUR=,F10.2,3HDEG)
241     TSUR=TSUR+273.16
C
243     SIG=5.70E-12*DX*DY
246     READ(5,300)ITYPE
300     FORMAT(I5)
253     IF(ITYPE.LE.0) GO TO 301
C       OBS NEXT STATEMENT READS TWO CARDS
255     READ(5,2)CD,CKA,CKB,CMA,CMB,CPA,CPB,CPC,CB,CW,CTC,CPRES,CMV
312     WRITE(6,302)ITYPE,
1       CD,CKA,CKB,CMA,CMB,CPA,CPB,CPC,CB,CW,CTC,CPRES,CMV
302     FORMAT(6H0TYPE=,I2,12H GAS-COOLING/
16H DIAM=,9X,F10.2,2HCM/

```

HEAT

212H HEAT COND.=,8X,2E10.3,9HW/CM.DEG./  
311H VISCOSITY=,9X,2E10.3,4HPOIS/  
44H CP=,16X,3E10.3,8HJ/G.DEG./15H VOL.EXP.COEF.=,5X,E10.3/  
511H FLOW-RATE=,9X,E10.3,5HG/SEC/  
615H ENTERING TEMP=,F10.2,5HDEG.C/  
710H PRESSURE=,7X,F10.4,3HATA/  
812H MOL.WEIGHT=,4X,F10.3)

353 CTC=CTC+273.16

354 GT=CTC

355 GO TO 303

356 301 WRITE(6,304) I TYPE

304 FORMAT(6H0TYPE=,I2,7H VACUUM)

364 303 CONTINUE

C

364 READ(5,7)MX,(AX(I),BX(I),EX(I),I=1,MX)

7 FORMAT(I5/(3F10.0))

410 WRITE(6,8)(I,AX(I),BX(I),EX(I),I=1,MX)

8 FORMAT(8HORX-FUNC/(I,X,I3,2F10.5,F11.2))

C

434 READ(5,7)MY,(AY(I),BY(I),EY(I),I=1,MY)

460 WRITE(6,9)(I,AY(I),BY(I),EY(I),I=1,MY)

9 FORMAT(8HORY-FUNC/(I,X,I3,2F10.5,F11.2))

C

504 READ(5,7)MZ,(AZ(I),BZ(I),EZ(I),I=1,MZ)

530 WRITE(6,10)(I,AZ(I),BZ(I),EZ(I),I=1,MZ)

10 FORMAT(8HORZ-FUNC/(I,X,I3,2F10.5,F11.2))

C

554 READ(5,7)MC,(AC(I),BC(I),DC(I),I=1,MC)

70 FORMAT(I5/(3F10.0))

600 WRITE(6,11)(I,AC(I),BC(I),DC(I),I=1,MC)

11 FORMAT(8HOC-FUNC/(I,X,I3,2F10.5,F11.2))

C

624 READ(5,12)IM,JM,KM

12 FORMAT(3I5)

636 LM=3

637 IF(KM.EQ.1) LM=LM-1

642 IF(JM.EQ.1) LM=LM-1

645 IF(IM.EQ.1) LM=LM-1

650 WRITE(6,13)IM,JM,KM,LM

13 FORMAT(1H0,2(I3,2H X),I3,2H =,I2,12H DIMENSIONAL)

664 XM=DY\*DZ/DX

666 YM=DX\*DZ/DY

667 ZM=DX\*DY/DZ

670 VM=0.

671 IF(DT.GT.0.) VM=DX\*DY\*DZ/DT

676 TIME=0.

677 POINTS=0.

700 14 READ(5,15)I,J,K,NCIJK,NRIJK,NGIJK,TIJK,QIJK,FIJK,CXIJK,CYIJK,CZIKK

15 FORMAT(6I3,2X,6F10.0)

734 IF(I.LE.0) GO TO 16

736 IF(I.GT.IM) GO TO 14

741 IF(J.GT.JM) GO TO 14

744 IF(K.GT.KM) GO TO 14

753 POINTS=POINTS+QIJK

755 TIJK=TIJK+TADD

757 T(I,J,K)=TIJK

HEAT

757		TG(I,J,K)=TIJK
760		Q(I,J,K)=QIJK
761		F(I,J,K)=FIJK
763		CX(I,J,K)=CXIJK
764		CY(I,J,K)=CYIJK
766		CZ(I,J,K)=CZIJK
767		NC(I,J,K)=NCIJK
771		NR(I,J,K)=NRIJK
772		NG(I,J,K)=NGIJK
774		GO TO 14
	C	
775	16	WRITE(6,17)
	17	FORMAT(5HODATA/2H T/2H Q/2H F/3H CT/3H RT/3H CX/3H CY/3H CZ)
1001		IF(ITYPE.EQ.1) WRITE(6,170)
	170	FORMAT(3H NG)
1007		WRITE(6,753)POINTS
	753	FORMAT(1H0,F12.5,7H POINTS)
	C	
1015		DO 18 K=1,KM
1017		WRITE(6,5)(PT(I),I=1,15),IVERS,MODIF
1030		WRITE(6,19)K,TIME,ITER
	19	FORMAT(6HOLAYER,I3,8H AT TIME,F10.5,3HSEC,I5,4HITER)
1042		WRITE(6,20)(I,I=1,IM)
	20	FORMAT(3HOX=,3X,10I10)
1055		DO 18 J=1,JM
1057		WRITE(6,21)J,(T(I,J,K),I=1,IM)
	21	FORMAT(3HOY=,I3,10F10.2)
1073		WRITE(6,22)(Q(I,J,K),I=1,IM)
	22	FORMAT(6X,10F10.2)
1106		IF(GSIGE.EQ.0.0) GO TO 5433
1107		DO 5432 I=1,IM
1111		IF(F(I,J,K))5431,5432,5432
1117	5431	F(I,J,K)=F(I,J,K)*GSIGE
1125	5432	CONTINUE
1130	5433	CONTINUE
1130		WRITE(6,22)(F(I,J,K),I=1,IM)
1143		WRITE(6,23)(NC(I,J,K),I=1,IM)
	23	FORMAT(4X,10I10)
1156		WRITE(6,23)(NR(I,J,K),I=1,IM)
1171		WRITE(6,22)(CX(I,J,K),I=1,IM)
1204		WRITE(6,22)(CY(I,J,K),I=1,IM)
1217		WRITE(6,22)(CZ(I,J,K),I=1,IM)
1232		IF(ITYPE.EQ.1) WRITE(6,23)(NG(I,J,K),I=1,IM)
1247		DO 120 I=1,IM
1251		IF(F(I,J,K))121,121,120
1257	121	IF(NC(I,J,K).LT.1) WRITE(6,150)I,J,K
	150	FORMAT(3HONC,3I5//)
1277		IF(NR(I,J,K).LT.1) WRITE(6,151)I,J,K
	151	FORMAT(3HONR,3I5//)
1317		RKT=RKT+0.0001
1321	120	CONTINUE
1324		DO 24 I=1,IM
	C	RECALCULATE CURRENT IN PULSE FROM PULSE-TIME AND MEAN-CURRENT
1340		Q(I,J,K)=Q(I,J,K)*UA*PA*(TOFF+TON)/TON
1344		T(I,J,K)=T(I,J,K)+273.16
1346	24	TG(I,J,K)=T(I,J,K)



HEAT

1350	18	CONTINUE
1355		ION=1
1355		TSW=TON
1357	25	ITER=-1
1360		TSUR4=TSUR**4
1362	26	CONTINUE
	C	GAUSS-SIEDEL ITERATION CYCLE STARTS
1362		IF(ITYPE.EQ.0) GO TO 3100
1363		QTG=0.
1364		CK=SUD(CKA,CKB,GT)
1366		GMU=SUD(CMA,CMB,GT)
1371		CR=CMV*CPRES/(82.054*GT)
1375		CP=POL(CPA,CPB,CPC,GT)
1401		CONA=CK*DX*DY*1.62*(1.273*CW*CP/(CK*CD))**0.33333
1413		CONB=3.375E-6*CD**3*CR**2*CB*980.665
1420	3100	CONTINUE
1420		ITER=ITER+1
1422		SUM=0.
1423		DO 30 I=1,IM
1424		DO 30 J=1,JM
1425		DO 30 K=1,KM
1426		DTA=0.
1427		DNA=0.
1427		IF(F(I,J,K))31,32,30
1436	31	DTA=DTA+SIG*F(I,J,K)*(T(I,J,K)**4-TSUR4)
1454		IF(ITYPE)32,32,306
1456	306	IF(NG(I,J,K))32,32,307
1464	307	GMUF=SUD(CMA,CMB,0.5*(GT+T(I,J,K)))
1504		QCG=CONA*(GMU/GMUF)**0.3333
1510		QCG=QCG*(1.+(CONB*(T(I,J,K)-GT)/GMU**2))**0.33333
	C	LIMIT THE GAS-COOLING TO MAX 1 SURFACE
1520		QCG=QCG*(T(I,J,K)-GT)*F(I,J,K)*0.5
1524		QTG=QTG+QCG
1526		DTA=DTA+QCG
1527	32	L=NC(I,J,K)
1534		CC=VM*POL(AC(L),BC(L),DC(L),T(I,J,K))
1544		IF(CC.LT.0.) CC=0.
1547		DTA=DTA+TG(I,J,K)*CC
1556		IF(ION.EQ.1) DTA=DTA+Q(I,J,K)
1573		DNA=CC
1574		L=NR(I,J,K)
1575		IF(LM.EQ.0) GO TO 74
1577		GO TO(41,42,43),LM
	C	TREAT Z-COORDINATE
1605	43	CC=ZM*CZ(I,J,K)*POL(AZ(L),BZ(L),EZ(L),T(I,J,K))
1624		IF(CC.LT.0.) CC=0.
1627		DNA=DNA+CC
1631		IF(K.EQ.1) GO TO 51
1633		M=NR(I,J,K-1)
1640		IF(M.EQ.0) GO TO 51
1641		CCM=ZM*CZ(I,J,K-1)*POL(AZ(M),BZ(M),EZ(M),T(I,J,K-1))
1657		IF(CCM.LT.0.) CCM=0.
1667		DTA=DTA+CCM*T(I,J,K-1)
1671		DNA=DNA+CCM
1673		GO TO 52
1700	51	DTA=DTA+CC*T(I,J,K)

HEAT

1703		DNA=DNA+CC
1704	52	IF(K.EQ.KM) GO TO 53
1706		DTA=DTA+CC*T(I,J,K+1)
1715		GO TO 42
1715	53	DTA=DTA+CC*T(I,J,K)
	C	TREAT Y-COORDINATE
1724	42	CC=YM*CY(I,J,K)*POL(AY(L),BY(L),EY(L),T(I,J,K))
1743		IF(CC.LT.0.) CC=0.
1746		DNA=DNA+CC
1750		IF(J.EQ.1) GO TO 61
1752		M=NR(I,J-1,K)
1756		IF(M.EQ.0) GO TO 61
1760		CCM=YM*CY(I,J-1,K)*POL(AY(M),BY(M),EY(M),T(I,J-1,K))
1775		IF(CCM.LT.0.) CCM=0.
2005		DTA=DTA+CCM*T(I,J-1,K)
2007		DNA=DNA+CCM
2011		GO TO 62
2016	61	DTA=DTA+CC*T(I,J,K)
2021		DNA=DNA+CC
2022	62	IF(J.EQ.JM) GO TO 63
2024		DTA=DTA+CC*T(I,J+1,K)
2033		GO TO 41
2033	63	DTA=DTA+CC*T(I,J,K)
	C	TREAT X-COORDINATE
2042	41	CC=XM*CX(2,4,K)*POL(AX(L),BX(L),EX(L),T(I,J,K))
2056		IF(CC.LT.0.) CC=0.
2061		DNA=DNA+CC
2063		IF(I.EQ.1) GO TO 71
2065		M=NR(I-1,J,K)
2072		IF(M.EQ.0) GO TO 71
2074		CCM=XM*CX(I-1,J,K)*POL(AX(M),BX(M),EX(M),T(I-1,J,K))
2110		IF(CCM.LT.0.) CCM=0.
2120		DTA=DTA+CCM*T(I-1,J,K)
2122		DNA=DNA+CCM
2124		GO TO 72
2131	71	DTA=DTA+CC*T(I,J,K)
2134		DNA=DNA+CC
2135	72	IF(I.EQ.IM) GO TO 73
2137		DTA=DTA+CC*T(I+1,J,K)
2146		GO TO 74
2146	73	DTA=DTA+CC*T(I,J,K)
2155	74	SU=-T(I,J,K)
2162		IF(DNA.EQ.0. .OR. DTA.GT.1.E+100) WRITE(6,75)I,J,K,ITER,DNA,DTA
	75	FORMAT(3H0**,4I5,2E15.4)
2217		T(I,J,K)=DTA/DNA
2221		SU=SU+T(I,J,K)
2223		SUM=SUM+ABS(SU)
2225		IF(T(I,J,K).GT.TMIT) GO TO 400
2235	30	CONTINUE
	C	
	C	CALCULATE NEW GAS MEAN-TEMPERATURE
2245		IF(ITYPE.EQ.1) GT=CTC-QTG/(CW*CP)
2252		IF(ITER.GE.1000) GO TO 1001
2255		IF(SUM.GT.RKT) GO TO 26
	C	
2260	1001	TIME=TIME+DT

HEAT

```
2262      DO 80 K=1,KM
2264      IF(TIME.LT.TMIN)GO TO 2000
2266      WRITE(6,5)(PT(I),I=1,15),IVERS,MODIF
2300      WRITE(6,3)UA,PA,TUN,TOFF,TMLT
2316      IF(DT.LE.0.) WRITE(6,90)K,ITER
2330      IF(DT.GT.0.) WRITE(6,19)K,TIME,ITER
          90      FORMAT(6HOLAYER,I3,12HSTEADY-STATE,I5,4HITER)
2343      2000      CONTINUE
2343      WRITE(6,404)
          404      FORMAT(1H )
2347      IF(ION) 101,101,102
2351      101      WRITE(6,105)
          105      FORMAT(9H+BEAM OFF)
2355      GO TO 103
2356      102      WRITE(6,106)
          106      FORMAT(8H+BEAM ON)
2362      103      CONTINUE
2362      IF(TIME.LT.TMIN)GO TO 2001
2365      WRITE(6,404)
2370      WRITE(6,20)(I,I=1,IM)
2403      2001      CONTINUE
2403      TMN=-1000.
2405      DO 80 J=1,JM
2406      DO 82 I=1,IM
2407      IF(F(I,J,K).GT.0.) GO TO 82
2416      IF(T(I,J,K).LT.TMN) GO TO 82
2427      TMN=T(I,J,K)
2430      IH=I
2430      JH=J
2431      KH=K
2433      82      PR(I)=T(I,J,K)-273.16
2444      IF(TIME.LT.TMIN)GO TO 2002
2447      WRITE(6,21)J,(PR(I),I=1,IM)
2457      2002      CONTINUE
2457      DO 81 I=1,IM
2461      PR(I)=-SIG*F(I,J,K)*T(I,J,K)**4
2474      PR(I)=PR(I)*1000.
2476      IF(F(I,J,K))81,81,83
2503      83      PR(I)=0.
2505      81      TG(I,J,K)=T(I,J,K)
2520      IF(TIME.LT.TMIN) GO TO 80
2522      WRITE(6,22)(PR(I),I=1,IM)
2531      IF(ITYPE) 80,80,315
2533      315      DO 310 I=1,IM
2535      IF(F(I,J,K))311,312,312
2543      311      IF(NG(I,J,K))312,312,313
2551      313      GMUF=SUD(CMA,CMB,0.5*(GT+T(I,J,K)))
2571      QCG=CONA*(GMU/GMUF)**0.33333
2575      QCG=QCG*(1.+(CONB*(T(I,J,K)-GT)/GMU**2)**0.3333)
2605      QCG=QCG*(T(I,J,K)-GT)*F(I,J,K)*0.5
2611      PR(I)=-QCG
2613      GO TO 310
2614      312      PR(I)=0.
2616      310      CONTINUE
2621      WRITE(6,22)(PR(I),I=1,IM)
2627      80      CONTINUE
```

HEAT

```
2634      IF(TIME.GE.TMIN) WRITE(6,404)
2643      IF(ITYPE.EQ.0) GO TO 321
2644      GTT=GT-273.16
2646      WRITE(6,320)GTT
          320      FORMAT(1H+,60X,15H GAS MEAN-TEMP=,F10.2,5HDEG.C)
2654      321      CONTINUE
2654      TMN=TMN-273.16
2656      WRITE(6,2005)TIME, TMN, IH, JH, KH, ITER
          2005      FORMAT(11X,7H T-MAX=,F10.5,F10.2,4I3)
2676      IF(DT.LE.0.) GO TO 1000
2700      IF(TIME.LT.TSW) GO TO 100
2702      IF(ION.EQ.1) TSW=TSW+TOFF
2706      IF(ION.NE.1) TSW=TSW+TON
2711      ION=-ION
2712      100      CONTINUE
2712      IF(TIME.LT.TMAX) GO TO 25
2715      GO TO 1000
          C      AN ELEMENT IS SO HOT THAT IT MELTS AWAY
2715      400      WRITE(6,401)I, J, K, ITER
          401      FORMAT(13H **MELTING AT,4I3,2H**)
2736      F(I, J, K)=1.
2737      T(I, J, K)=273.16
2741      CX(I, J, K)=0.
2741      CY(I, J, K)=0.
2742      CZ(I, J, K)=0.
2743      IF(I.GT.1)CX(I-1, J, K)=0.
2752      IF(J.GT.1) CY(I, J-1, K)=0.
2761      IF(K.GT.1) CZ(I, J, K-1)=0.
2770      GO TO 25
2771      END
```

APPENDIX 3. Example of the printout from program HEAT v4m1

1/2MIL 1CM DIAM AU-FOIL IN DOUBLE GAUSSIAN AT 1M/UA

HEAT VERS 4 MOD 1

BEAM= 4.000UA, POWER= 2.526E-03MEV/POINT TON= .0050S, TOFF= .0200S, MELTS AT T= 10000.00

DX= .06250CM, DY= .06250CM, DZ= .00127CM, DT= .00100SEC, TMAX= .22600SEC, TMIN= .20000SEC

TSUR= 20.00DEG

TYPE= 0 VACUUM

RX-FUNC

1	3.29400	-.00057	4183.00
2	1.64700	-.00028	2092.00
3	-0.00000	-0.00000	-0.00

RY-FUNC

1	3.29400	-.00057	4183.00
2	3.29400	-.00057	4183.00
3	1.64700	-.00028	2092.00

RZ-FUNC

1	-0.00000	-0.00000	-0.00
2	-0.00000	-0.00000	-0.00
3	-0.00000	-0.00000	-0.00

C-FUNC

1	2.31800	.00051	-0.00
2	1.15900	.00025	-0.00
3	.57950	.00013	-0.00

9 X 9 X 1 = 2 DIMENSIONAL

DATA

T  
Q  
F  
CT  
RT  
CX  
CY  
CZ

98.95750 POINTS

1/2MIL 1CM DIAM AU-FOIL IN DOUBLE GAUSSIAN AT 1M/UA

HEAT VERS 4 MOD 1

LAYER 1 AT TIME 0.00000SEC -1ITER

X=	1	2	3	4	5	6	7	8	9		
Y= 1	20.00	20.00	20.00	20.00	20.00	20.00	20.00	20.00	20.00	20.00	T(°C)
	0.00	.39	.97	1.66	2.00	1.66	.97	.39	.06		P(points)
	1.00	-.02	-.02	-.02	-.02	-.02	-.02	-.02	-.01		F
	2	2	2	2	2	2	2	2	3		Cp-type
	2	2	2	2	2	2	2	2	3		λ-type
	1.00	1.00	1.00	1.00	1.00	1.00	1.00	1.00	1.00		Cx
	1.00	1.00	1.00	1.00	1.00	1.00	1.00	1.00	1.00		Cy
	1.00	1.00	1.00	1.00	1.00	1.00	1.00	1.00	1.00		Cz
Y= 2	20.00	20.00	20.00	20.00	20.00	20.00	20.00	20.00	20.00	20.00	
	0.00	.74	1.82	3.22	3.98	3.52	2.28	1.23	.39		
	1.00	-.04	-.04	-.04	-.04	-.04	-.04	-.04	-.02		
	1	1	1	1	1	1	1	1	2		
	1	1	1	1	1	1	1	1	3		
	1.00	1.00	1.00	1.00	1.00	1.00	1.00	1.00	1.00		
	1.00	1.00	1.00	1.00	1.00	1.00	1.00	1.00	1.00		
	1.00	1.00	1.00	1.00	1.00	1.00	1.00	1.00	1.00		
Y= 3	0.00	20.00	20.00	20.00	20.00	20.00	20.00	20.00	20.00	20.00	
	0.00	0.00	1.52	2.82	3.82	3.89	3.12	2.28	.97		
	1.00	1.00	-.04	-.04	-.04	-.04	-.04	-.04	-.02		
	0	1	1	1	1	1	1	1	2		
	0	1	1	1	1	1	1	1	3		
	0.00	1.00	1.00	1.00	1.00	1.00	1.00	1.00	1.00		
	0.00	1.00	1.00	1.00	1.00	1.00	1.00	1.00	1.00		
	0.00	1.00	1.00	1.00	1.00	1.00	1.00	1.00	1.00		
Y= 4	0.00	20.00	20.00	20.00	20.00	20.00	20.00	20.00	20.00	20.00	
	0.00	0.00	1.08	2.18	3.34	3.95	3.89	3.52	1.66		
	1.00	1.00	-.04	-.04	-.04	-.04	-.04	-.04	-.02		
	0	1	1	1	1	1	1	1	2		
	0	1	1	1	1	1	1	1	3		
	0.00	1.00	1.00	1.00	1.00	1.00	1.00	1.00	1.00		
	0.00	1.00	1.00	1.00	1.00	1.00	1.00	1.00	1.00		
	0.00	1.00	1.00	1.00	1.00	1.00	1.00	1.00	1.00		
Y= 5	0.00	0.00	20.00	20.00	20.00	20.00	20.00	20.00	20.00	20.00	
	0.00	0.00	0.00	1.43	2.46	3.34	3.82	3.98	2.00		
	1.00	1.00	1.00	-.04	-.04	-.04	-.04	-.04	-.02		
	0	0	1	1	1	1	1	1	2		
	0	0	1	1	1	1	1	1	3		
	0.00	0.00	1.00	1.00	1.00	1.00	1.00	1.00	1.00		
	0.00	0.00	1.00	1.00	1.00	1.00	1.00	1.00	1.00		
	0.00	0.00	1.00	1.00	1.00	1.00	1.00	1.00	1.00		
Y= 6	0.00	0.00	20.00	20.00	20.00	20.00	20.00	20.00	20.00	20.00	
	0.00	0.00	0.00	.74	1.43	2.18	2.82	3.22	1.66		
	1.00	1.00	1.00	-.04	-.04	-.04	-.04	-.04	-.02		
	0	0	1	1	1	1	1	1	2		
	0	0	1	1	1	1	1	1	3		
	0.00	0.00	1.00	1.00	1.00	1.00	1.00	1.00	1.00		
	0.00	0.00	1.00	1.00	1.00	1.00	1.00	1.00	1.00		
	0.00	0.00	1.00	1.00	1.00	1.00	1.00	1.00	1.00		

Y= 7	0.00	0.00	0.00	20.00	20.00	20.00	20.00	20.00	20.00
	0.00	0.00	0.00	0.00	0.00	1.08	1.52	1.82	.97
	1.00	1.00	1.00	1.00	1.00	-.04	-.04	-.04	-.02
	0	0	0	1	1	1	1	1	2
	0	0	0	1	1	1	1	1	3
	0.00	0.00	0.00	1.00	1.00	1.00	1.00	1.00	1.00
	0.00	0.00	0.00	1.00	1.00	1.00	1.00	1.00	1.00
	0.00	0.00	0.00	1.00	1.00	1.00	1.00	1.00	1.00
Y= 8	0.00	0.00	0.00	0.00	0.00	20.00	20.00	20.00	20.00
	0.00	0.00	0.00	0.00	0.00	0.00	0.00	.74	.39
	1.00	1.00	1.00	1.00	1.00	1.00	1.00	-.04	-.02
	0	0	0	0	0	1	1	1	2
	0	0	0	0	0	1	1	1	3
	0.00	0.00	0.00	0.00	0.00	1.00	1.00	1.00	1.00
	0.00	0.00	0.00	0.00	0.00	1.00	1.00	1.00	1.00
	0.00	0.00	0.00	0.00	0.00	1.00	1.00	1.00	1.00
Y= 9	0.00	0.00	0.00	0.00	0.00	0.00	0.00	20.00	20.00
	0.00	0.00	0.00	0.00	0.00	0.00	0.00	0.00	0.00
	1.00	1.00	1.00	1.00	1.00	1.00	1.00	1.00	1.00
	0	0	0	0	0	0	0	1	2
	0	0	0	0	0	0	0	1	3
	0.00	0.00	0.00	0.00	0.00	0.00	0.00	1.00	1.00
	0.00	0.00	0.00	0.00	0.00	0.00	0.00	1.00	1.00
	0.00	0.00	0.00	0.00	0.00	0.00	0.00	1.00	1.00

BEAM ON	T-MAX=	.00100	35.03	9	5	1	13
BEAM ON	T-MAX=	.00200	48.89	9	5	1	13
BEAM ON	T-MAX=	.00300	61.79	9	5	1	13
BEAM ON	T-MAX=	.00400	73.87	9	5	1	13
BEAM ON	T-MAX=	.00500	85.43	7	4	1	13
BEAM OFF	T-MAX=	.00600	81.82	7	4	1	11
BEAM OFF	T-MAX=	.00700	78.67	7	4	1	10
BEAM OFF	T-MAX=	.00800	76.19	8	4	1	10
BEAM OFF	T-MAX=	.00900	74.25	9	4	1	10
BEAM OFF	T-MAX=	.01000	72.61	9	4	1	11
BEAM OFF	T-MAX=	.01100	71.25	8	3	1	11
BEAM OFF	T-MAX=	.01200	70.45	9	3	1	11
BEAM OFF	T-MAX=	.01300	69.80	8	2	1	11
BEAM OFF	T-MAX=	.01400	69.44	9	2	1	11
BEAM OFF	T-MAX=	.01500	69.20	9	1	1	11
BEAM OFF	T-MAX=	.01600	68.75	9	1	1	11
BEAM OFF	T-MAX=	.01700	68.14	9	1	1	11

1/2MIL ICM DIAM AU-FOIL IN DOUBLE GAUSSIAN AT 1W/UA

HEAT VERS 4 MOD 1

BEAM= 4.000UA, POWER= 2.526E-03MEV/POINT TON= .0050S, TOFF= .0200S, MELTS AT T= 10000.00

LAYER 1 AT TIME .20100SEC 11ITER

BEAM OFF

X=	1	2	3	4	5	6	7	8	9	
Y= 1	20.00 0.00	29.60 .00	41.95 .00	55.33 .01	68.07 .01	78.95 .01	87.17 .01	92.24 .01	93.96 .00	T(°C) P <sub>radiated</sub> (mW)
Y= 2	20.00 0.00	27.67 .01	40.18 .01	53.68 .01	66.42 .01	77.28 .01	85.47 .01	90.54 .02	92.25 .01	
Y= 3	0.00 0.00	20.00 0.00	35.13 .01	49.03 .01	61.67 .01	72.36 .01	80.45 .01	85.48 .01	87.18 .01	
Y= 4	0.00 0.00	20.00 0.00	29.65 .01	42.38 .01	54.32 .01	64.55 .01	72.38 .01	77.30 .01	78.98 .01	
Y= 5	0.00 0.00	0.00 0.00	20.00 0.00	34.00 .01	44.86 .01	54.32 .01	61.68 .01	66.45 .01	68.10 .01	
Y= 6	0.00 0.00	0.00 0.00	20.00 0.00	27.21 .01	34.01 .01	42.38 .01	49.04 .01	53.69 .01	55.34 .01	
Y= 7	0.00 0.00	0.00 0.00	0.00 0.00	20.00 0.00	20.00 0.00	29.64 .01	35.14 .01	40.18 .01	41.95 .00	
Y= 8	0.00 0.00	0.00 0.00	0.00 0.00	0.00 0.00	0.00 0.00	20.00 0.00	20.00 0.00	27.65 .01	29.58 .00	
Y= 9	0.00 0.00	0.00 0.00	0.00 0.00	0.00 0.00	0.00 0.00	0.00 0.00	0.00 0.00	20.00 0.00	20.00 0.00	
T-MAX=	.20100		93.96	9	1	1	11			



Table I. Approximate grayness factors (g) for some common materials (data from Ref. 7).  
 O = oxidized, U = unoxidized.

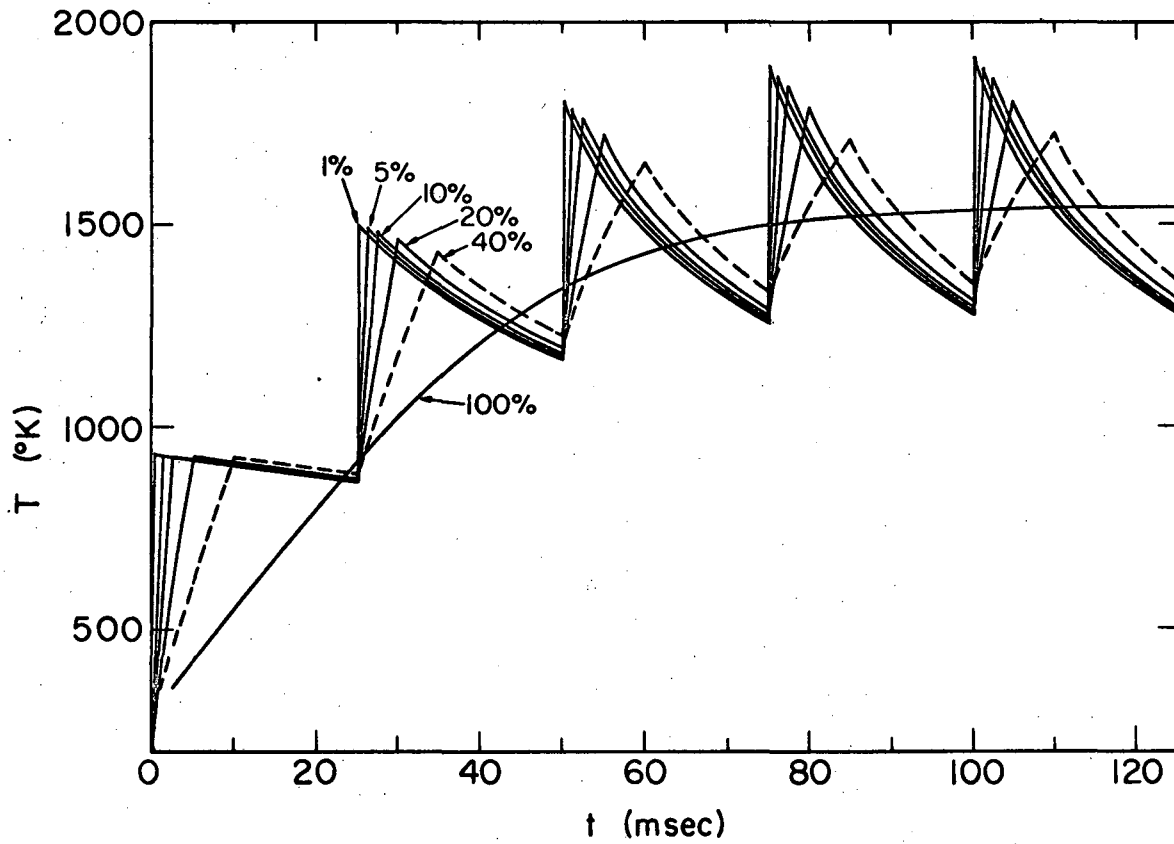
Material	Surface	25° C	100° C	200° C	500° C	600° C	1000° C	1200° C	1500° C
Aluminum	U	0.022	0.028		0.060				
	O			0.11		0.19			
Bismuth	U	0.048	0.061						
Brass	U	0.035	0.035						
	O			0.61		0.59			
Carbon	U	0.81	0.81		0.79				
Chromium	U		0.08						
Cobalt	U				0.13		0.23		
Niobium	U								0.19
Copper	U		0.02						
	O			0.6			0.6		
Gold	U		0.02		0.03				
Iron	U		0.05						
	O		0.74		0.84			0.89	
Lead	U		0.05						
	O			0.63					
Monel	O			0.43		0.43			
Mercury	U	0.10	0.12						
Molybdenum	U						0.13		0.19
Nickel	U	0.045	0.06		0.12		0.19		
	O			0.37				0.85	
Platinum	U	0.037	0.047		0.096		0.152		0.191
Silica	Amorph.						0.80	0.85	
Silver	U		0.02		0.035				
Steel	U		0.08						
	O	0.80		0.79		0.79			
Tantalum	U								0.21
Tin	U	0.043	0.05						
Tungsten	U	0.024	0.032		0.071		0.15		0.23
Zinc	U	0.05							

Table II. Coefficients in the polynomial approximation of the heat conductivity,  $\lambda = a + bT + c/T^2$ , with T in °K and  $\lambda$  in W/cm degree.

Material	a	b	c	Range (°K)	Max. deviation (%)
Aluminum	2.501	$-4.184 \cdot 10^{-4}$	$1.114 \cdot 10^4$	15-920	+30/-15
Beryllium	1.893	$-9.897 \cdot 10^{-4}$	$1.316 \cdot 10^4$	20-1250	+72/-18
Bismuth	0.03162	$1.091 \cdot 10^{-4}$	$4.308 \cdot 10^2$	70-1070	+22/-26
Cadmium	1.495	$-1.537 \cdot 10^{-3}$	$-2.368 \cdot 10^3$	86-673	+16/-10
Chromium	1.116	$-4.421 \cdot 10^{-4}$	$2.192 \cdot 10^3$	20-1200	+39/-14
Cobalt	2.098	$-4.883 \cdot 10^{-3}$	$1.909 \cdot 10^3$	25-293	+10.7/-6.1
Copper	4.416	$-9.729 \cdot 10^{-4}$	$9.236 \cdot 10^3$	20-1280	+32/-9
Germanium, single cryst.	0.8568	$-1.135 \cdot 10^{-3}$	$7.142 \cdot 10^3$	30-370	+4.1/-5.8
Gold	3.294	$-5.697 \cdot 10^{-4}$	$4.183 \cdot 10^3$	30-1300	+3.5/-3.5
Graphite	0.1405	$4.557 \cdot 10^{-5}$	$2.163 \cdot 10^5$	293-2273	+1.5/-1.6
Iridium	0.8179	$1.232 \cdot 10^{-3}$	$9.477 \cdot 10^3$	24-500	+13/-8
Iron	0.9106	$-6.042 \cdot 10^{-4}$	$3.934 \cdot 10^3$	20-1040	+32/-18
Lead	0.1079	$5.539 \cdot 10^{-5}$	$2.025 \cdot 10^4$	293-1073	+28/-20
Magnesium	1.891	$-8.682 \cdot 10^{-4}$	$4.285 \cdot 10^3$	19-1073	+28/-13
Manganese	-1.143	$9.842 \cdot 10^3$	$1.975 \cdot 10^3$	56-273	---
Mercury	0.02104	$1.221 \cdot 10^{-4}$	$3.360 \cdot 10^3$	83-1070	+53/-21
Molybdenum	1.467	$-3.465 \cdot 10^{-4}$	$2.435 \cdot 10^3$	33-1910	+5.8/-7.6
Nickel	0.5272	$4.078 \cdot 10^{-5}$	$2.401 \cdot 10^3$	33-1620	+38/-24
Niobium	0.4277	$1.347 \cdot 10^{-4}$	$5.718 \cdot 10^2$	30-1900	+10/-6
Palladium	0.1035	$1.837 \cdot 10^{-3}$	$2.390 \cdot 10^3$	30-373	+9.9/-7.1
Platinum	0.6327	$1.307 \cdot 10^{-4}$	$1.347 \cdot 10^3$	12-2000	+6.0/-4.0
Rhenium	0.4242	$5.748 \cdot 10^{-5}$	$2.347 \cdot 10^3$	30-500	+12/-10
Rhodium	1.903	$-1.110 \cdot 10^{-3}$	$1.879 \cdot 10^2$	10-500	+2.1/-3.4
Selenium, single cryst.	0.02174	$-2.714 \cdot 10^{-7}$	$1.658 \cdot 10^2$	25-400	+13/-14
Silicon, single cryst.	0.9443	$-5.277 \cdot 10^{-4}$	$8.166 \cdot 10^3$	23-1400	+72/-43
Silver	5.334	$-2.454 \cdot 10^{-3}$	$6.717 \cdot 10^3$	15-800	+14/-5.5
Tantalum	0.4709	$6.250 \cdot 10^{-5}$	$1.878 \cdot 10^2$	30-2500	+18/-8
Thorium	0.2298	$2.227 \cdot 10^{-4}$	$-3.261 \cdot 10^2$	300-580	---
Tin	0.2287	$3.867 \cdot 10^{-5}$	$3.478 \cdot 10^4$	293-773	+22/-10
Titanium	0.2934	$-1.245 \cdot 10^{-4}$	$-2.398 \cdot 10^1$	10-800	+22/-17
Tungsten	1.453	$-1.801 \cdot 10^{-4}$	$7.139 \cdot 10^3$	30-3500	+17/-9
Uranium	0.1884	$2.433 \cdot 10^{-4}$	$-3.047 \cdot 10^1$	20-1070	+7.5/-6.2
Vanadium	0.2870	$9.620 \cdot 10^{-5}$	$-9.041 \cdot 10^1$	20-1173	+2.0/-1.3
Zinc	1.256	$-4.509 \cdot 10^{-4}$	$-2.037 \cdot 10^2$	73-673	+0.5/-0.3
Zirconium	0.3256	$-1.364 \cdot 10^{-4}$	$2.143 \cdot 10^2$	36-600	+1.3/-1.9

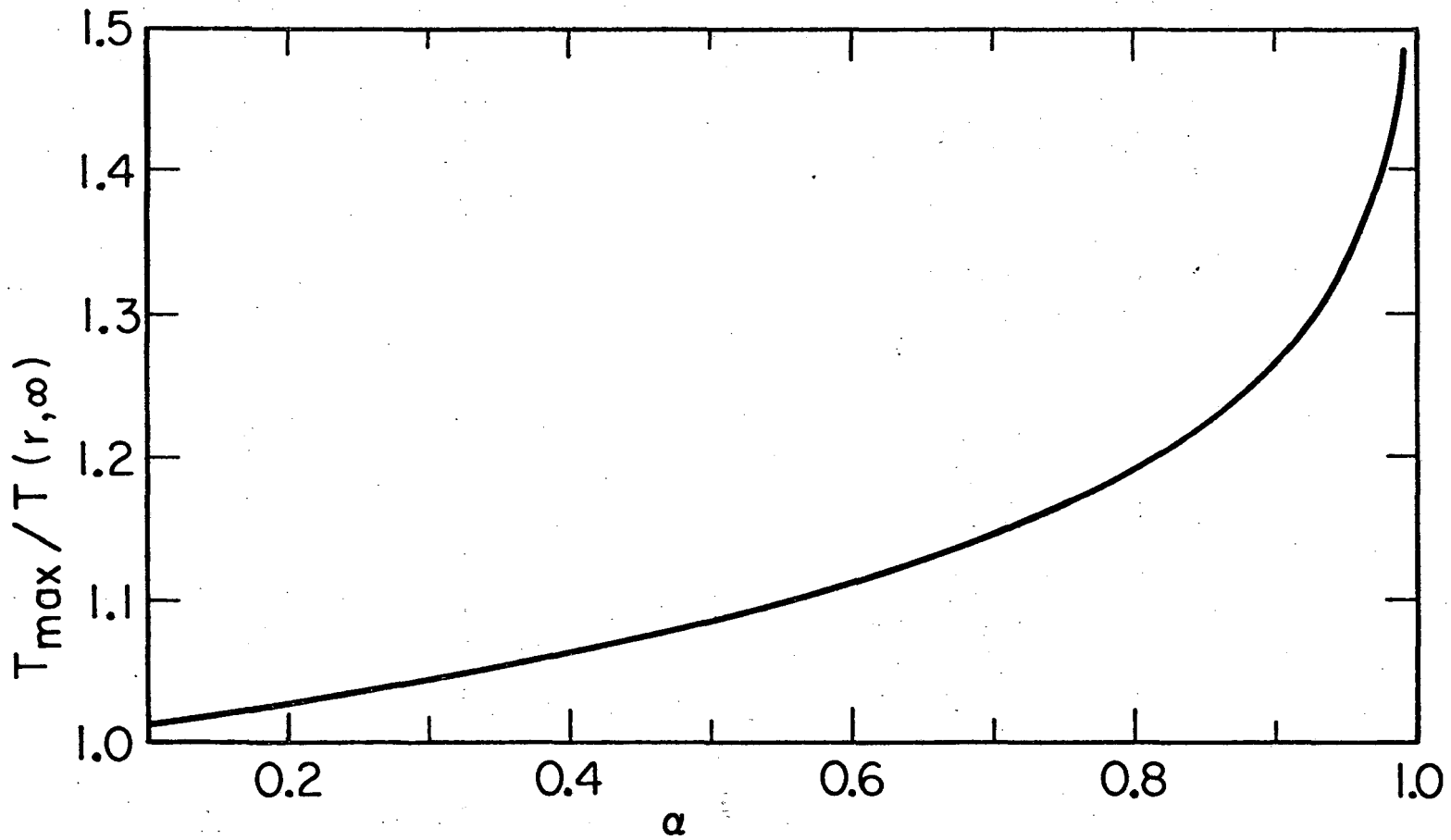
Table III. Coefficients in the polynomial approximation of the heat capacity,  $C_p = a + bT + c/T^2$ , with T in °K and  $C_p$  in J/ml degree. Values recalculated from Ref. 8.

Material	a	b	c	Range (°K)
Aluminum	2.061	$1.235 \cdot 10^{-3}$	---	298-932
Antimony	1.266	$4.000 \cdot 10^{-4}$	---	298-903
Arsenic, metallic	1.67	$7.09 \cdot 10^{-4}$	---	298-1100
Beryllium	2.902	$2.475 \cdot 10^{-3}$	---	298-1300
Bismuth	0.881	$1.059 \cdot 10^{-3}$	---	298-544
Cadmium	1.707	$9.45 \cdot 10^{-4}$	---	298-594
Calcium	0.8478	$5.50 \cdot 10^{-4}$	---	298-673
Chromium	0.3336	$1.348 \cdot 10^{-3}$	$-5.026 \cdot 10^4$	298-1823
Cobalt	2.949	$2.686 \cdot 10^{-3}$	---	298-718
Copper	3.181	$8.82 \cdot 10^{-4}$	---	298-1357
Germanium, cryst.	1.837	$3.519 \cdot 10^{-4}$	---	298-1213
Gold	2.318	$5.075 \cdot 10^{-4}$	---	298-1336
Graphite	3.219	$8.007 \cdot 10^{-4}$	$-1.649 \cdot 10^5$	298-2300
Iridium	2.702	$6.905 \cdot 10^{-4}$	---	298-1223
Iron	1.985	$4.181 \cdot 10^{-3}$	$2.53 \cdot 10^4$	298-1033
Lead	1.332	$4.354 \cdot 10^{-4}$	---	298-600
Magnesium	1.837	$4.49 \cdot 10^{-4}$	$-2.33 \cdot 10^4$	298-923
Manganese	3.126	$1.854 \cdot 10^{-3}$	$-2.03 \cdot 10^4$	298-1000
Mercury	1.868	---	---	298-634
Molybdenum	2.438	$5.78 \cdot 10^{-4}$	---	298-1800
Nickel	2.576	$4.467 \cdot 10^{-3}$	---	298-633
Niobium	2.183	$3.703 \cdot 10^{-4}$	---	298-1900
Palladium	2.604	$6.194 \cdot 10^{-4}$	---	298-1828
Platinum	2.629	$6.13 \cdot 10^{-4}$	---	298-1800
Rhenium	2.833	---	---	298
Rhodium	2.768	$1.039 \cdot 10^{-3}$	---	298-1900
Selenium, cryst.	1.55	---	---	298
Silicon, cryst.	2.071	$2.016 \cdot 10^{-4}$	$-3.912 \cdot 10^4$	298-1200
Silver	2.073	$8.31 \cdot 10^{-4}$	$1.47 \cdot 10^4$	298-1234
Tantalum	2.234	$2.988 \cdot 10^{-4}$	---	298-1900
Thorium	1.292	$6.182 \cdot 10^{-4}$	$7.05 \cdot 10^3$	298-1500
Tin	1.139	$1.624 \cdot 10^{-3}$	---	298-505
Titanium	2.064	$9.904 \cdot 10^{-4}$	---	298-1150
Tungsten	2.52	$3.34 \cdot 10^{-4}$	---	298-2000
Uranium	1.115	$2.635 \cdot 10^{-4}$	$2.3 \cdot 10^4$	298-935
Vanadium	2.598	$9.622 \cdot 10^{-4}$	---	298-1900
Zinc, metallic	2.445	$1.097 \cdot 10^{-3}$	---	298-692
Zirconium	1.276	$1.240 \cdot 10^{-3}$	$1.678 \cdot 10^4$	298-900



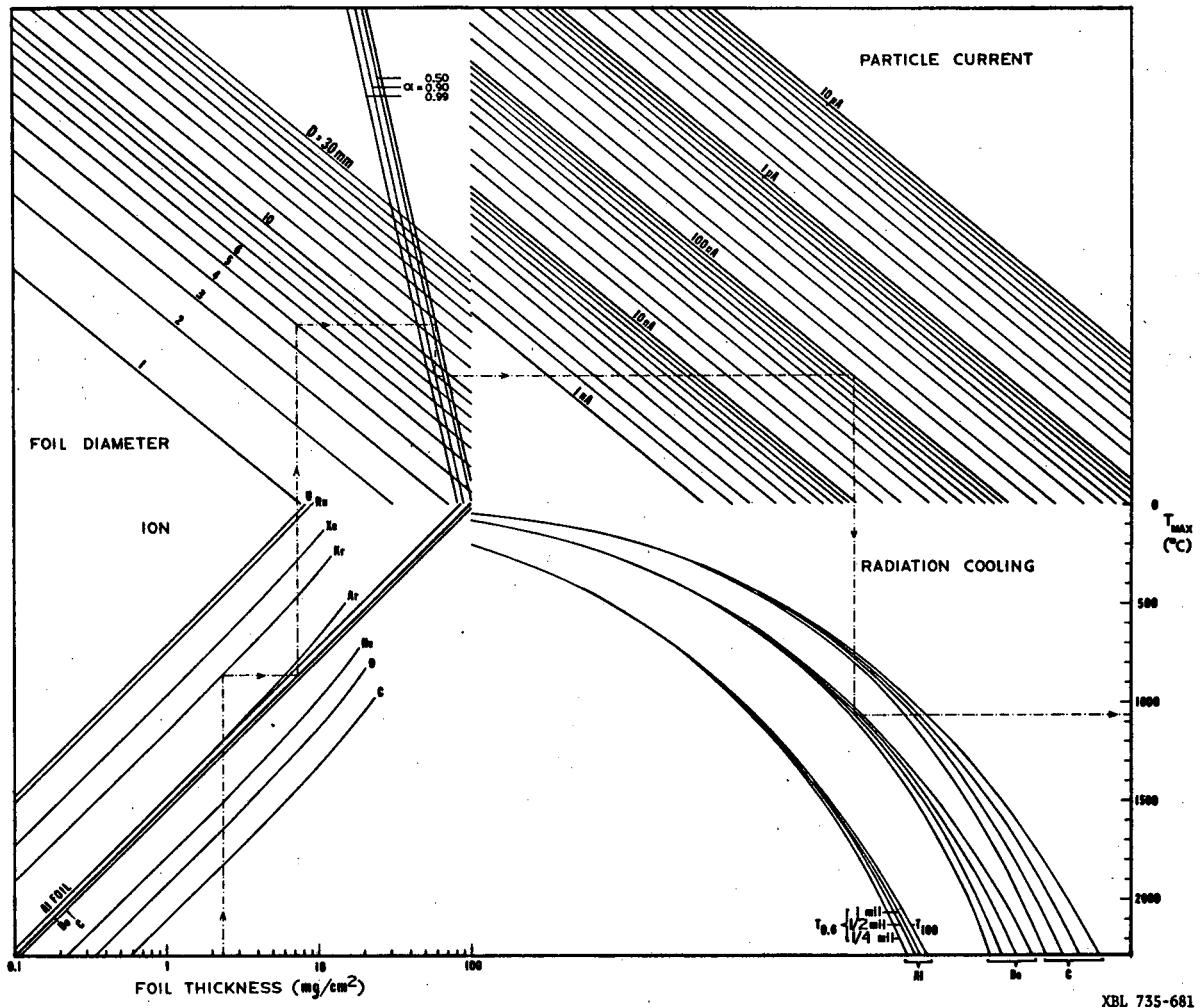
XBL736-3111

Fig. 1. Pure radiation cooling at different duty cycles [Eq. (39)];  $\frac{1}{4}$  mil ( $\sim 1.4 \text{ mg/cm}^2$ ) carbon foil at  $51 \text{ W/cm}^2$ .



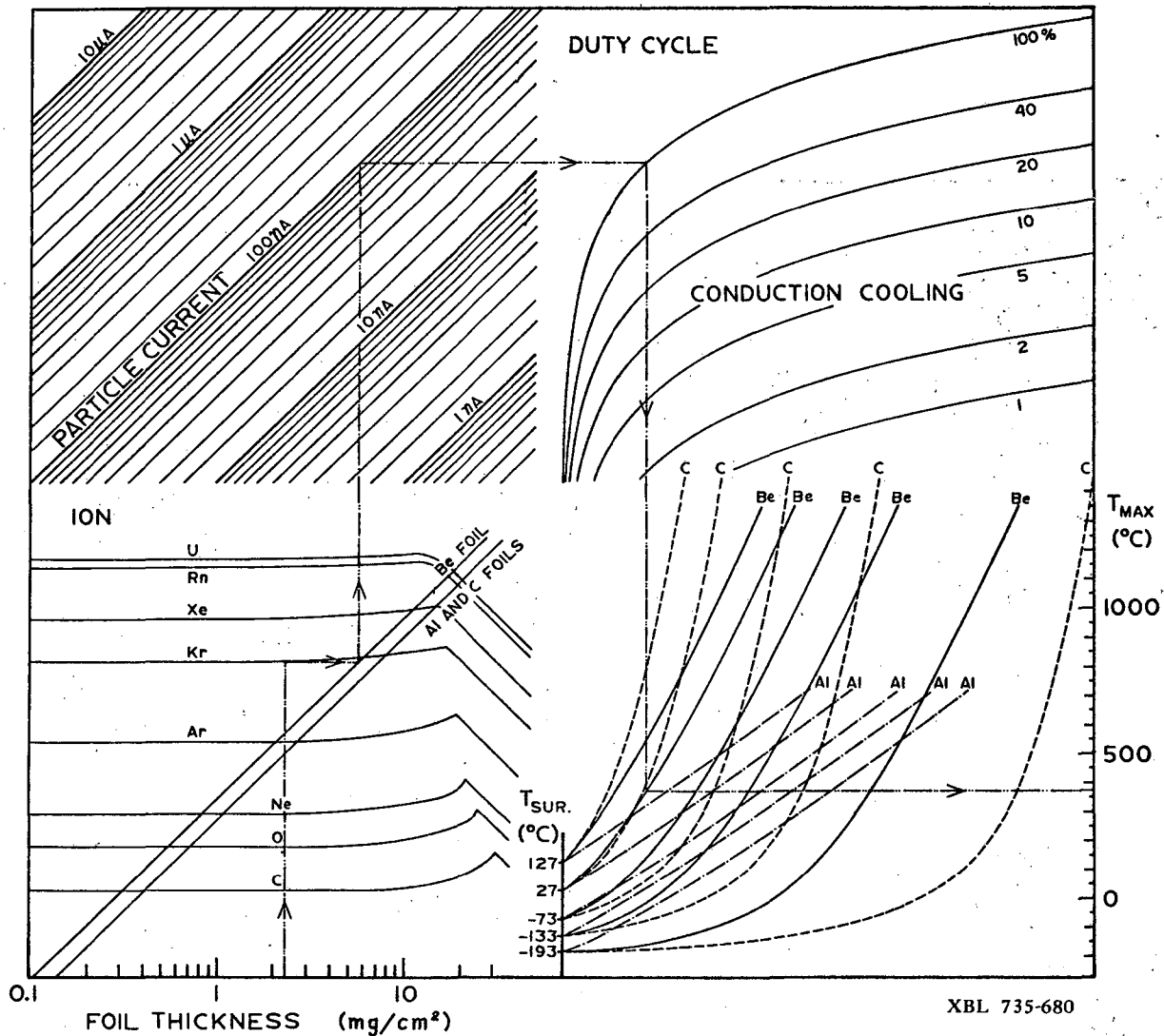
XBL736-3112

Fig. 2. The temperature ratio between Gaussian and uniform beams as a function of the fraction,  $\alpha$ , of the beam which is focused on the foil.



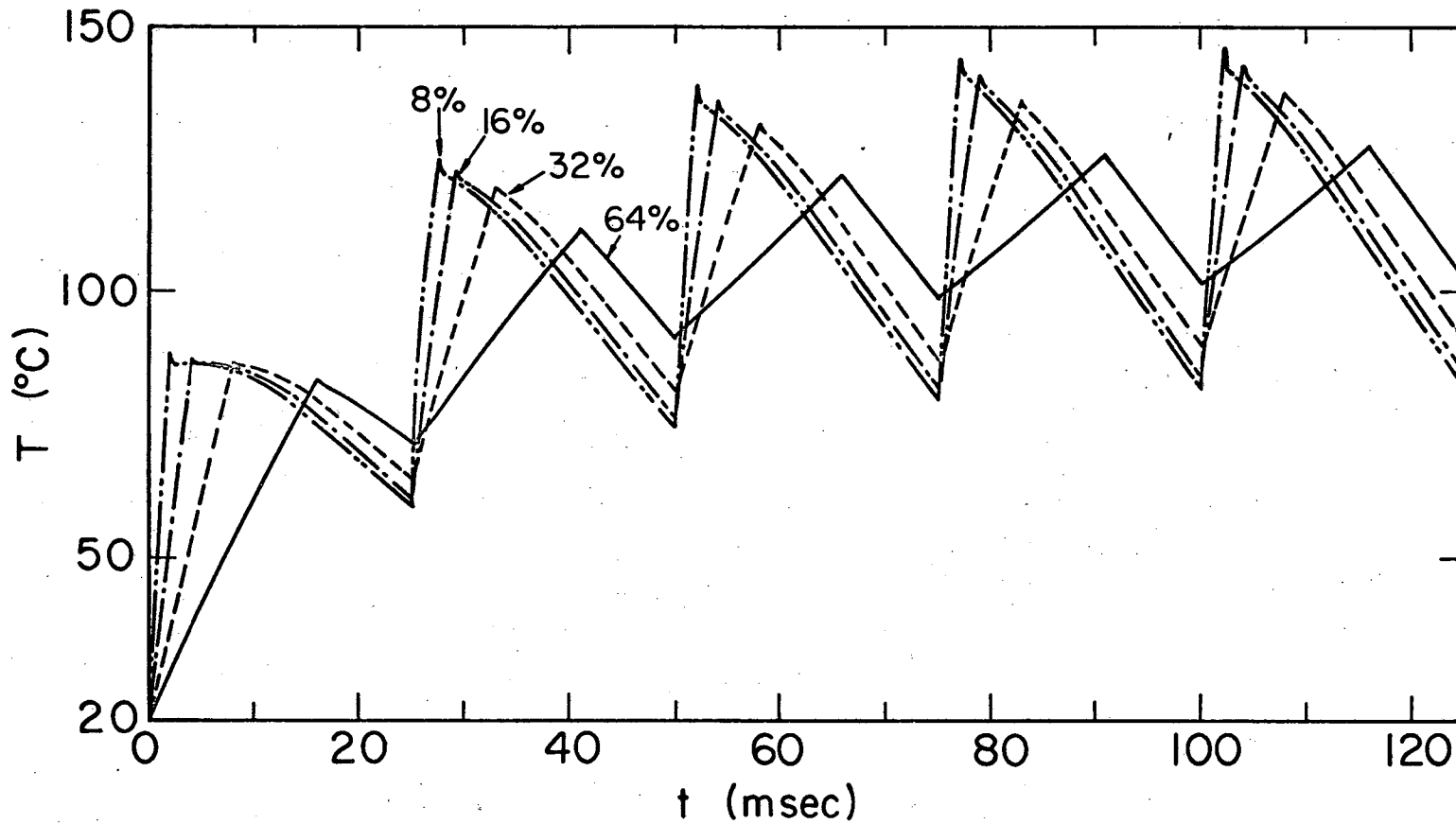
XBL 735-681

Fig. 3. Nomograph for evaluation of foil temperatures at 7.5 MeV/amu incident beam energy and pure radiation cooling. The nomograph is constructed for beryllium, aluminum, and carbon foils, and it consists of four quadrants. In the first quadrant the total dissipated power per current unit is evaluated from foil thickness, ion beam, and material. In the second quadrant the maximal power load per surface and current unit is evaluated from the total power, the foil diameter, and the fraction,  $\alpha$ , of a Gaussian beam hitting the foil. The correction for  $\alpha$  should be omitted for a uniform beam. In the third quadrant the maximal power per surface unit is evaluated from the beam current (particle current), and in the fourth quadrant the foil temperature is evaluated from the material and duty cycle (in percent).



XBL 735-680

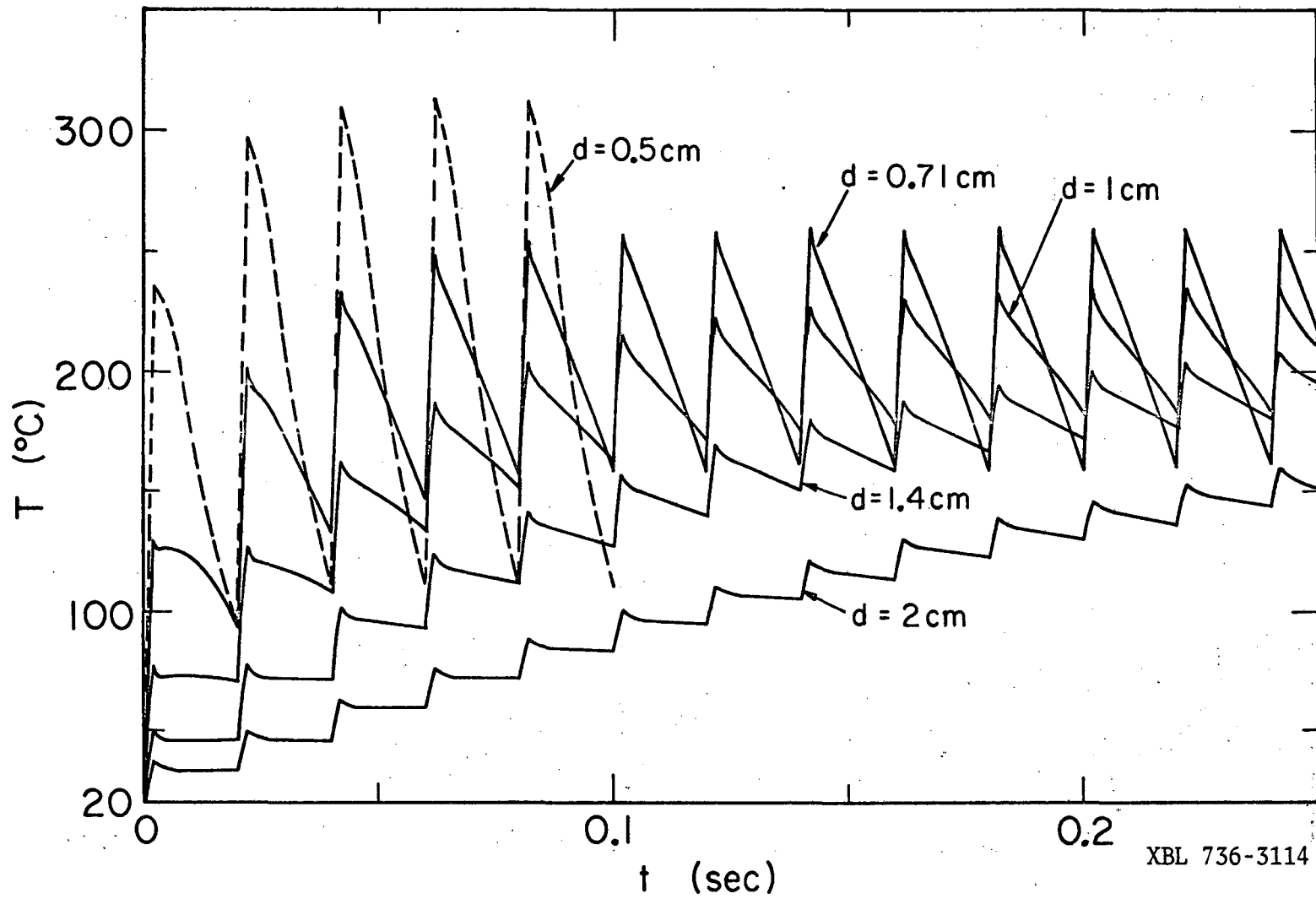
Fig. 4. Nomograph for the evaluation of foil temperatures at 7.5 MeV/amu incident beam energy, uniform beam shape, and pure conduction cooling. A first-order correction for Gaussian beam shape can be made as follows. First obtain the correction factor  $\psi/\alpha$  from Fig. 8, then read off the temperature for uniform beam shape, subtract  $T_{sur}$ , multiply the remainder by  $\psi/\alpha$  and add  $T_{sur}$  again. The nomograph is constructed for beryllium, aluminum, and carbon foils and it consists of four quadrants. In the first quadrant the power per unit thickness and current is evaluated from the foil thickness, ion beam, and foil material. This is converted in the second quadrant to power per unit thickness by multiplication with the beam current. The third quadrant involves mainly a change of scale from logarithmic to linear but it also corrects for the duty cycle. The curves are to be used for foils where the foil diameter (cm) is smaller than  $\sqrt{0.05 c \lambda / f \rho C_p}$ , where  $c$  is the duty cycle (percent),  $\lambda$  is the heat conductivity (W/cm degree)  $f$  is the beam pulse frequency (Hz),  $\rho$  is the density ( $\text{g/cm}^3$ ) and  $C_p$  is the heat capacity ( $\text{J/cm}^3$  degree). In the fourth quadrant the maximum temperature is evaluated from the edge temperature and material.



XBL736-3113

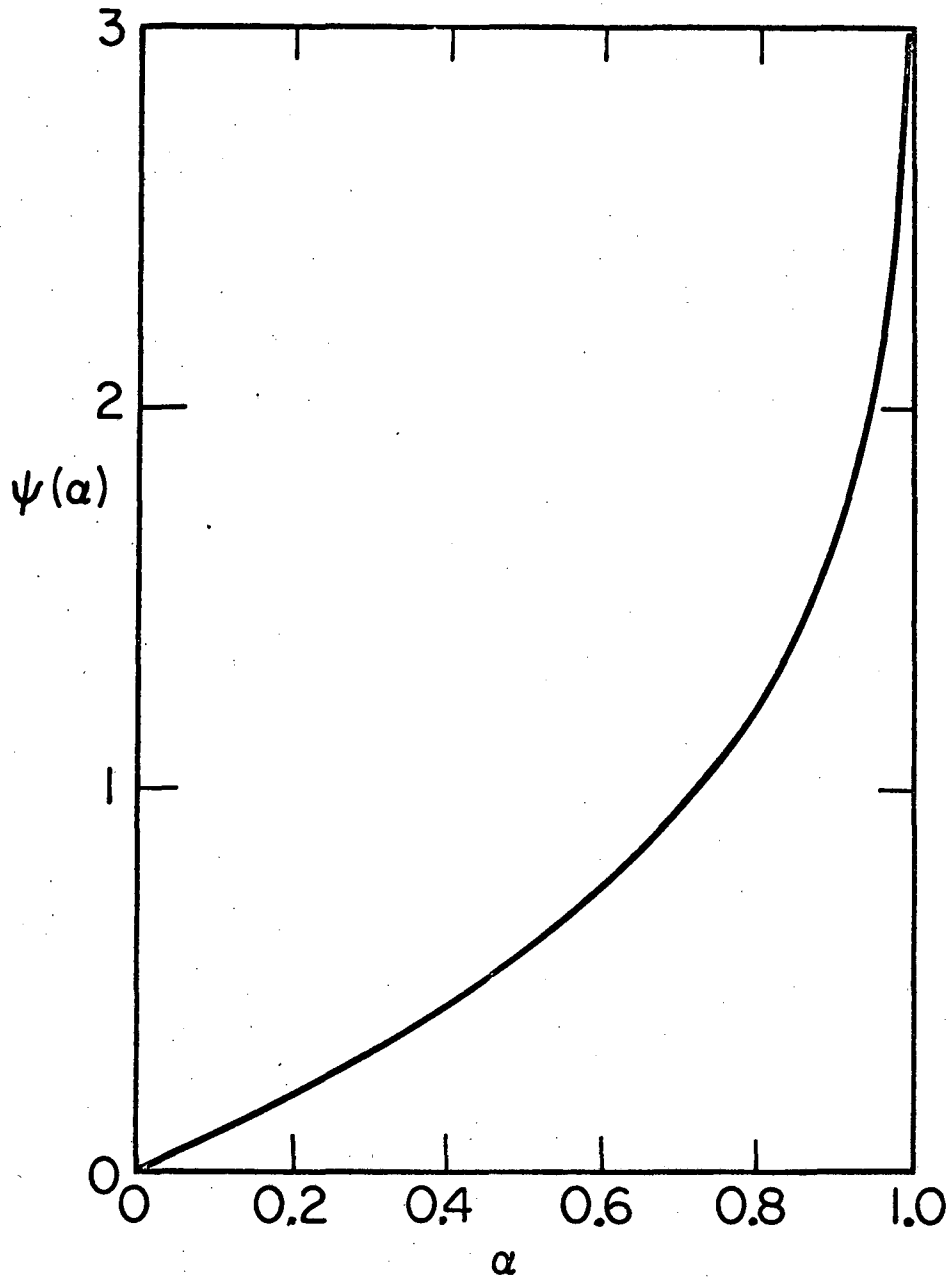
Fig. 5. Pure conduction cooling at different duty cycles [Eq. (56)];  $\frac{1}{2}$ -mil, 0.71-mm diameter aluminum foil at  $3.18 \text{ W/cm}^2$ .





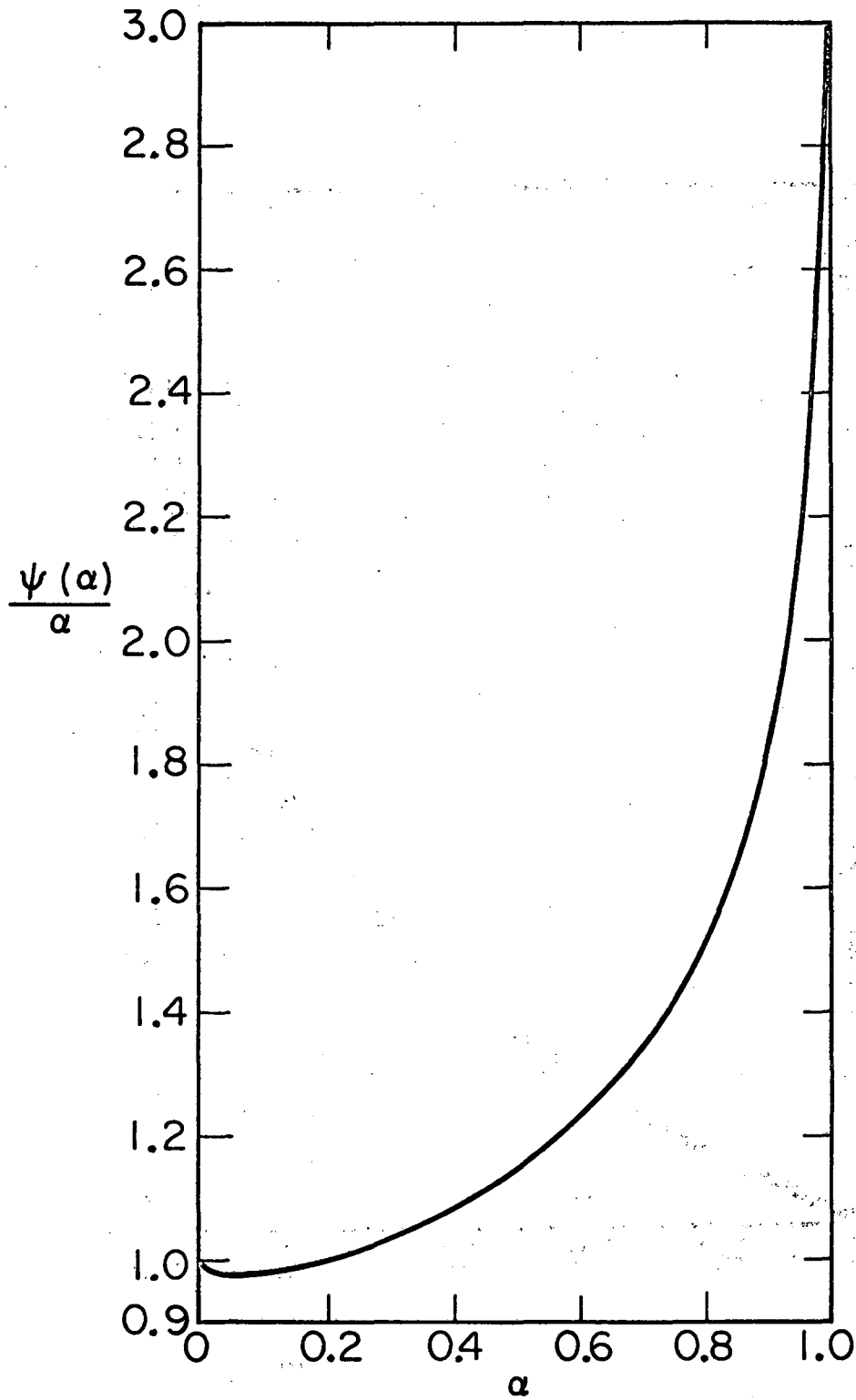
XBL 736-3114

Fig. 6. Variation of the center temperature with time for  $\frac{1}{2}$ -mil circular aluminum foils of 2, 1.4, 1.0, 0.71 and 0.5 cm diameter at a frequency of 50 Hz and a duty cycle of 10%.



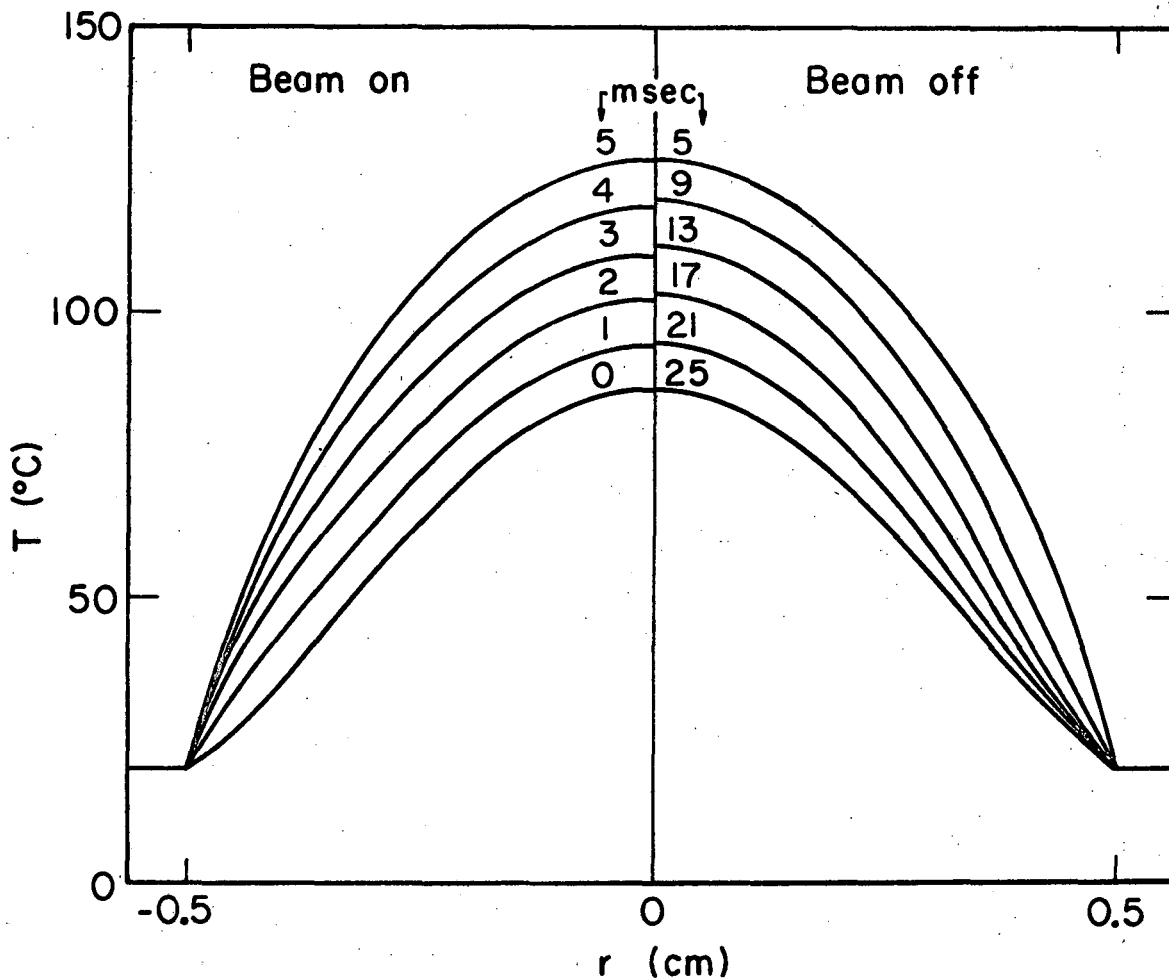
XBL736-3115

Fig. 7. The multiplier,  $\psi$ , for Gaussian beam shape and conduction-cooled foils as a function of the fraction,  $\alpha$ , of the beam focused on the foil [see Eq. (61)].



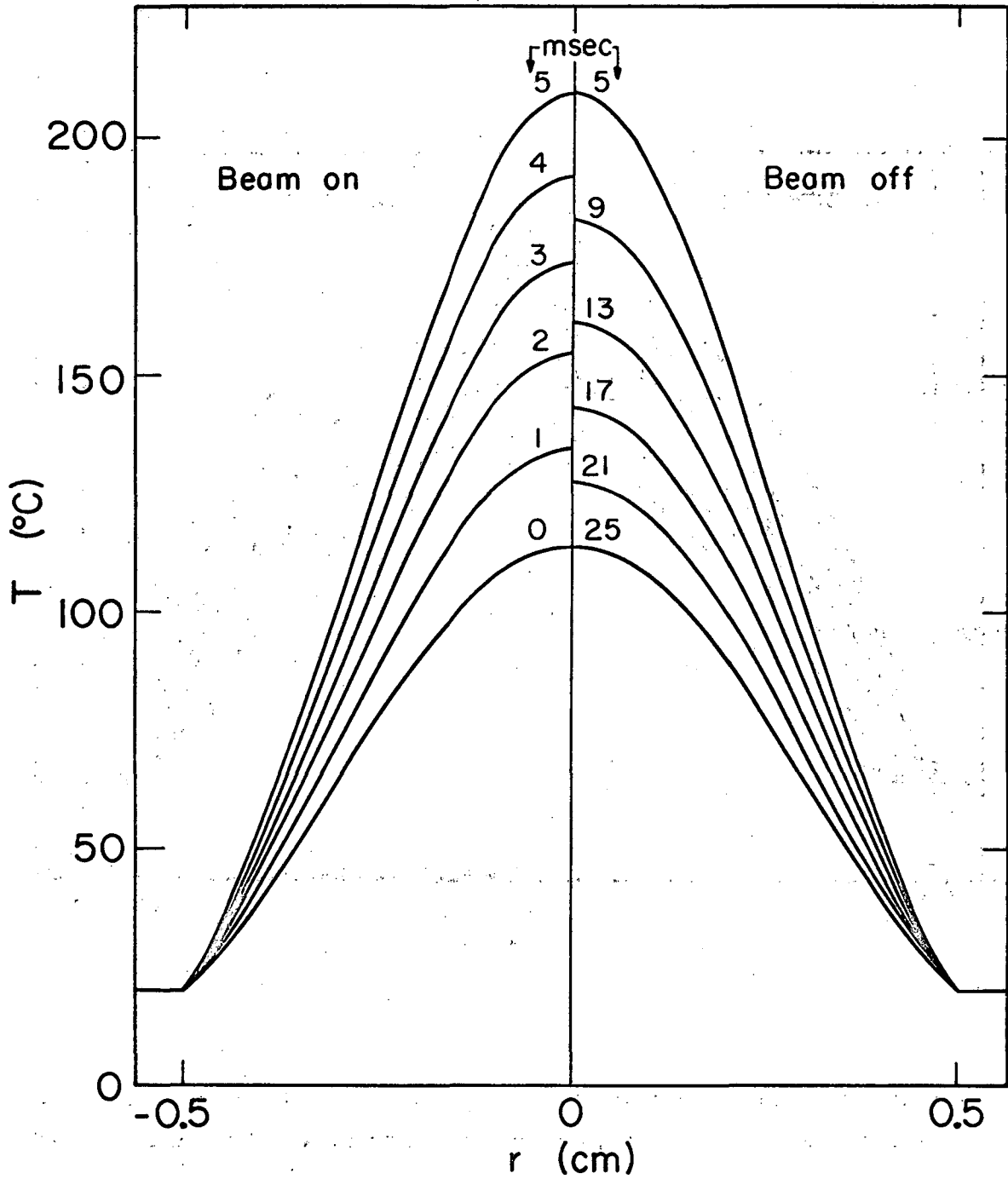
XBL736-3116

Fig. 8. The multiplier  $\psi/\alpha$  for Gaussian beam shape and conduction-cooled foils as a function of the beam fraction,  $\alpha$ , focused on the foil [see Eq. (62)].



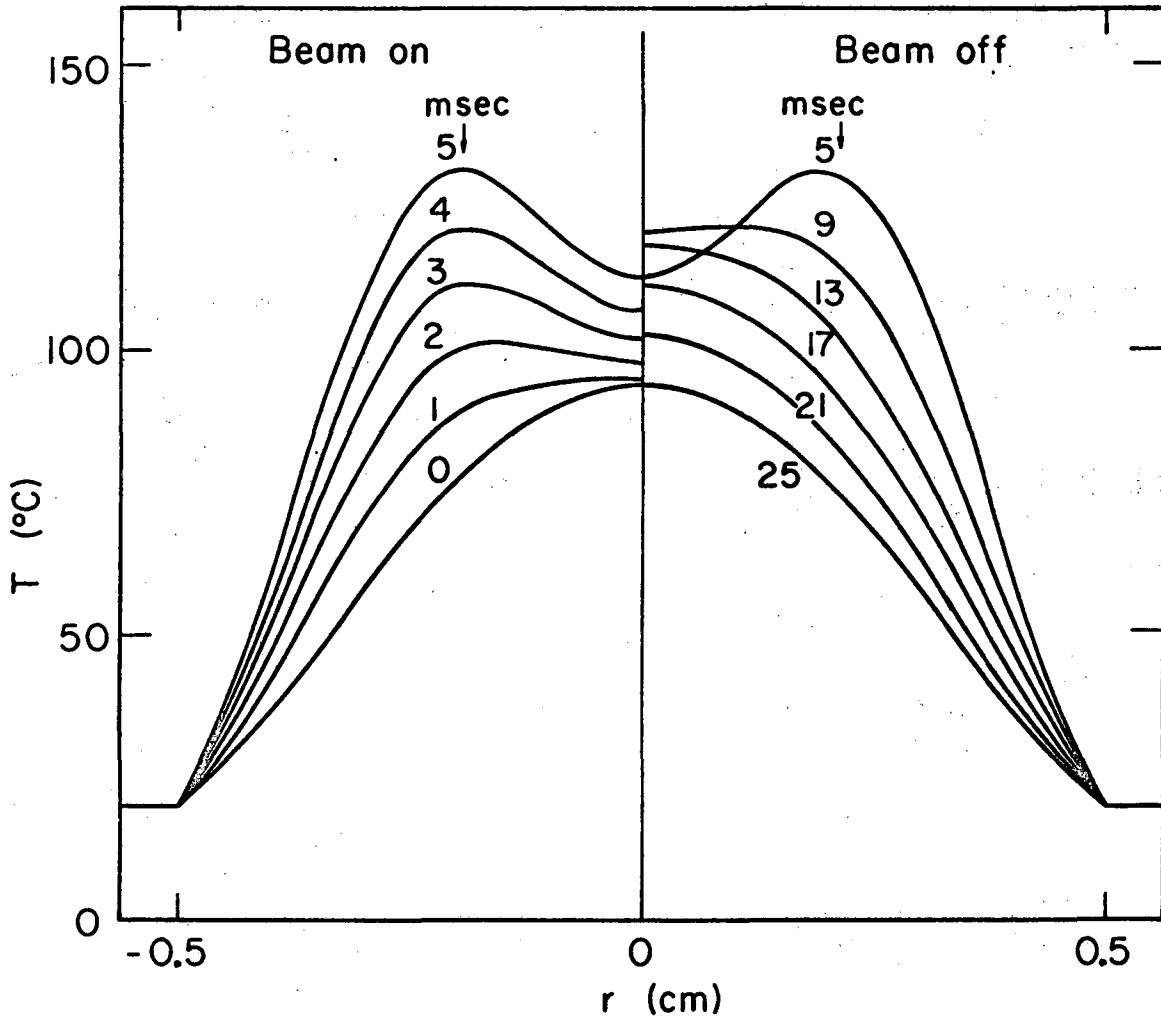
XBL736-3117

Fig. 9.  $\frac{1}{2}$ -mil, 1-cm-diameter gold foil in a pulsed uniform beam and a total dissipated power of 4W at a frequency of 40Hz and a duty cycle of 20%.



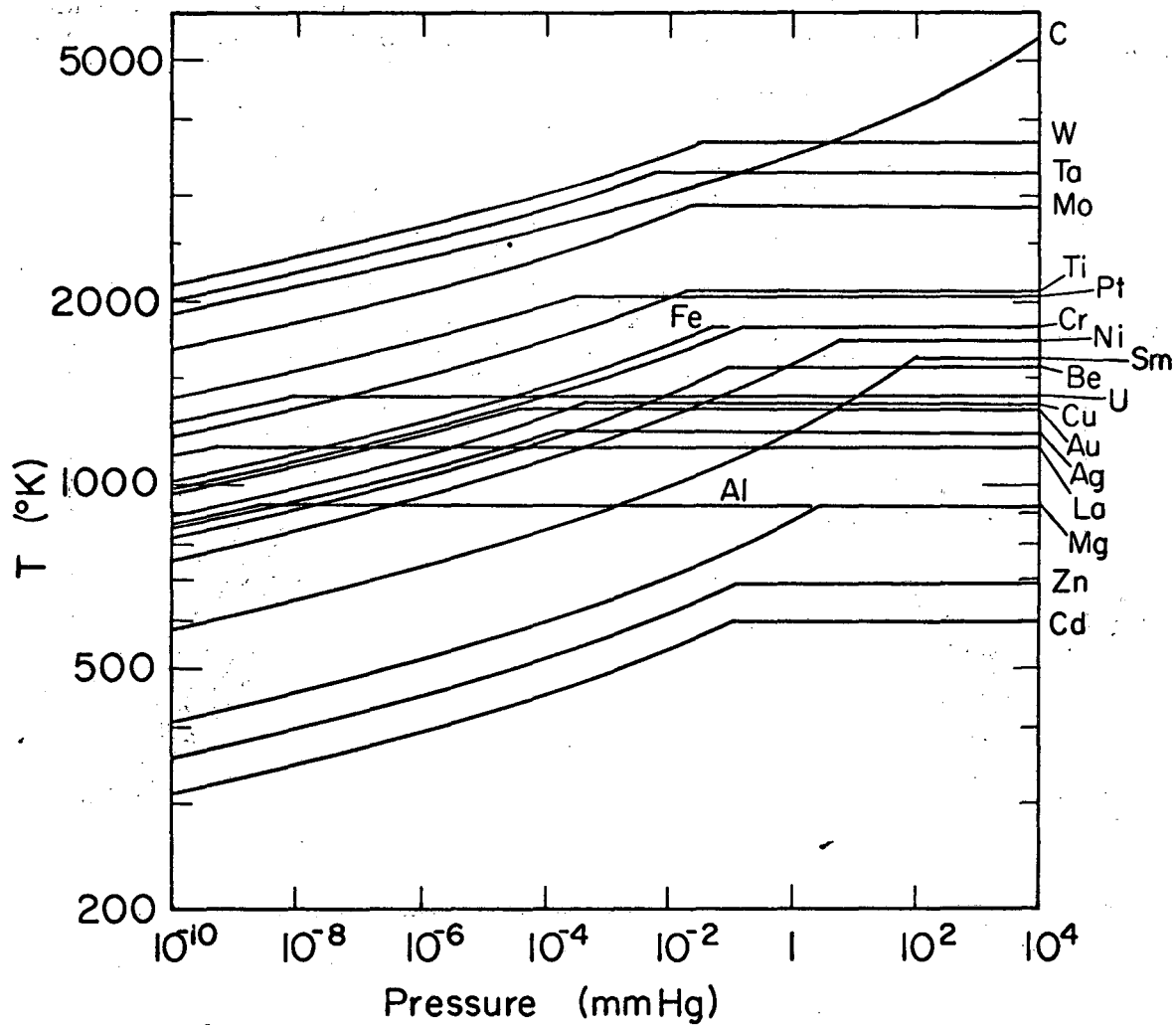
XBL736-3118

Fig. 10.  $\frac{1}{2}$ -mil, 1-cm-diameter gold foil in a pulsed Gaussian beam at a total dissipated power of 4W, a frequency of 40Hz and a duty cycle of 20%.



XBL 736-3119

Fig. 11.  $\frac{1}{2}$ -mil, 1-cm-diameter gold foil in a pulsed double-Gaussian beam at a total dissipated power of 4W, a frequency of 40Hz and a duty cycle of 20%.



XBL736-3120

Fig. 12. Temperature limits for material as a function of pressure. At high pressure the limit is set by the melting point and at low pressure by the vapor pressure.

LEGAL NOTICE

*This report was prepared as an account of work sponsored by the United States Government. Neither the United States nor the United States Atomic Energy Commission, nor any of their employees, nor any of their contractors, subcontractors, or their employees, makes any warranty, express or implied, or assumes any legal liability or responsibility for the accuracy, completeness or usefulness of any information, apparatus, product or process disclosed, or represents that its use would not infringe privately owned rights.*



TECHNICAL INFORMATION DIVISION  
LAWRENCE BERKELEY LABORATORY  
UNIVERSITY OF CALIFORNIA  
BERKELEY, CALIFORNIA 94720